To the Graduate Council:

I am submitting herewith a thesis written by Janel C. Holland entitled "Substrate Tolerance Studies of R67 Dihydrofolate Reductase". I have examined the final copy of this thesis for form and content and recommend that it be accepted in partial fulfillment of the requirements for the degree of Master of Science, with a major in Biochemistry.

Elizabeth E. Howell

Elizabeth E. Howell, Major Professor

We have read this thesis and recommend its acceptance:

Cynthia B. Peterson

[illegible]

Accepted for the Council:

C W Minkel

Associate Vice Chancellor
and Dean of The Graduate School

STATEMENT OF PERMISSION TO USE

In presenting this thesis in partial fulfillment of the requirements for a Master's degree at The University of Tennessee, Knoxville, I agree that the Library shall make it available to borrowers under the rules of the Library. Brief quotations from this thesis are allowable without special permission, provided that accurate acknowledgment of the source is made.

Permission for extensive quotation from or reproduction of this thesis may be granted by my major professor, or in her absence, by the Head of Interlibrary Services when, in the opinion of either, the proposed use of the material is for scholarly purposes. Any copying or use of the material in this thesis for financial gain shall not be allowed without my written permission.

Signature Jamel C. Holland

Date August 20, 1993

SUBSTRATE TOLERANCE STUDIES OF R67 DIHYDROFOLATE REDUCTASE

A Thesis

Presented for the

Master of Science

Degree

The University of Tennessee, Knoxville

Janel C. Holland

December 1993

DEDICATION

To my parents, Donald and Patricia, who have given me both love and strength, without which this degree would not have been possible.

ACKNOWLEDGEMENTS

I would like to thank my major professor, Dr. Elizabeth E. Howell, for her guidance and patience over the course of this project. I would also like to thank my other committee members, Dr. Cynthia B. Peterson, and Dr. Jorge Churchich, for their patience and assistance. I would like to express my thanks to Charles E. Linn for his indispensable laboratory and computer assistance over the past three years. Thanks to my fellow graduate students, Ping Zhaung, Guisheng Zhang, Amanda Dion, and Heonjong Park for their friendship and support. And finally, a special thanks to Dr. Robert Villafane, Celeste Shibata, Lisa Reece, and Robert J. Nichols, for without their advice and support I would have never been able to finish my degree.

ABSTRACT

R67 Dihydrofolate reductase (DHFR) is a plasmid encoded DHFR which confers a high level of resistance upon host bacterial cells to the antimicrobial drug trimethoprim (TMP). R67 DHFR shares no sequence or structural homology with the wildtype (wt.) *E. coli* chromosmal DHFR yet the two enzymes carry out identical reactions. The R-plasmid encoded enzyme is active as a homo-tetramer which is held together mainly by hydrophobic interactions which occur at the dimer-dimer interface. An interesting feature of R67 DHFR is that all four monomers share in the formation of the active site pore which is found in the center of the protein as an 18 A long pore with openings at both ends. The mechanism of R67 DHFR is not well understood; However it is thought to occur by binding a protonated substrate and the cofactor NADPH in the center of the active site pore.

To begin to determine R67 DHFR origins, and to investigate any functional similarity of R67 DHFR to wt. *E. coli* DHFR, substrate tolerance and ligand binding studies were performed. These studies show that R67 DHFR has a broader range of substrate tolerance and can bind more types of ligands than its chromosomal counterpart wt. *E.coli* DHFR. The results from this study also suggest that R67 DHFR could not have originated from any of the chromosomally encoded DHFRs, and

possibily that R67 DHFR is a primitive enzyme which was elicited by bacteria to reduce a wide variety of substrates quickly.

This study also describes experiments which involve two genetically engineered R67 DHFRs, an artificially duplicated monomer, R67 $DHFR_{double}$, and H62C R67 DHFR. Both of these enzymes have been engineered with the goal of breaking the unique symmetry of the enzyme and also to increase enzyme stability at lower pH. The results from these studies have shown that, in the case of the R67 $DHFR_{double}$, we have shown that the engineered R67 $DHFR_{double}$ protein is as active as native R67 DHFR. The results from the studies of the H62C R67 DHFR protein show that the protein is kinetically and fluorometrically different from the native enzyme. H62C R67 DHFR has also been shown to possess the ability to utilize acetyl-pyridine $NADP^+$ and NADPH to perform a transhydrogenase reaction, which is not present in the native R67 DHFR.

TABLE OF CONTENTS

	PAGE
CHAPTER I :	
BACKGROUND	1
CHAPTER II :	
SUBSTRATE TOLERANCE STUDIES WITH R67 DHFR	11
CHAPTER III :	
VARIANT LIGAND BINDING STUDIES WITH R67 DHFR	32
CHAPTER IV :	
STUDIES OF THE ARTIFICIALLY ENGINEERED R67 $DHFR_{double}$ ...	41
CHAPTER V :	
KINETIC STUDY OF THE ABILITY OF H62C R67 DHFR TO UTILIZE ACETYL-PYRIDINE $NADP^+$ IN A TRANSHYDROGENASE REACTION	46
CHAPTER VI:	
SUMMARY OF STUDY	50
LIST OF REFERENCES	54
APPENDIX	59
VITA	94

LIST OF FIGURES

FIGURE		PAGE
1.	Crystal structure of R67 DHFR dimeric form	60
2.	Tetrameric structure of R67 DHFR	61
3.	Proposed reaction mechanism of R67 DHFR for the reduction of DHF.....	62
4.	Oxidation/reduction of THP and generation/degradation of a-DMP at pH 7.0	63
5.	Crystal structure of DHPR	64
6.	Proposed mechanism for the MTHFR catalyzed reduction of MTHF	65
7.	Absorbance scans from the generation of q-DMP ...	66
8.	Absorbance scans of MTHF	67
9.	Absorbance scans of MeTHF	68
10.	Absorbance scans for the formation of FTHF	69
11.	Absorbance scans of sepiapterin	70
12.	Michaelis-Menten kinetics from the R67 DHFR catalyzed reduction of DHF	71
13.	Michaelis-Menten subsaturating kinetics from the R67 DHFR catalyzed reduction of q-DMP	72
14.	Michaelis-Menten subsaturating kinetics from the R67 DHFR catalyzed reduction of MTHF	73
15.	Michaelis-Menten subsaturating kinetics from the R67 DHFR catalyzed reduction of DHB	74
16.	Michaelis-Menten subsaturating kinetics from the R67 DHFR catalyzed reduction of DCPIP	75
17.	Michaelis-Menten kinetics from the R67 DHFR and wt. *E. coli* DHFR catalyzed reduction of DHB using NADPD or NADPH as the cofactor	76
18.	Absorbance scans of PLP-AMP	77

LIST OF FIGURES (continued)

FIGURE PAGE

19. Fluorescence quenching of tryptophan residues in R67 DHFR using FAD as the ligand 78

20. Fluorescence enhancement of the ligand FAD with R67 DHFR 79

21. Fluorescence quenching of tryptophan residues in R67 DHFR using FMN as the ligand 80

22. Fluorescence enhancement of the ligand FMN with R67 DHFR 81

23. Fluorescence quenching of tryptophan residues in R67 DHFR using PLP-AMP 82

24. Fluorescence quenching of typtophan residues in R67 DHFR using congo red as the ligand 83

25. Michaelis-Menten subsaturating kinetics from the R67 $DHFR_{double}$ catalyzed reduction of DHF 84

26. Fluorescence quenching of tryptophan residues in R67 $DHFR_{double}$ and R67 $DHFR_{native}$ using NADPH as the ligand 85

27. Michaelis-Menten kinetics from the R67 $DHFR_{double}$ and R67 $DHFR_{native}$ reduction of DHF using NADPD or NADPH as the cofactor 86

28. Michaelis-Menten subsaturating kinetics from H62C DHFR catalyzed reaction with acetyl-pyridine $NADP^+$ and NADPH 87

LIST OF TABLES

TABLE PAGE

1. Extinction coefficients and pKa values for DHF, q-DMP, and MTHF 88

2. Kinetic parameters for the R67 DHFR catalyzed reduction of DHF 88

3. Kinetic parameters for the R67 DHFR catalyzed reduction of q-DMP 89

4. Kinetic parameters for the R67 DHFR catalyzed reduction of MTHF 89

5. Kinetic parameters for the R67 DHFR catalyzed reduction of DHB 90

6. Kinetic parameters for the R67 DHFR catalyzed reduction of DCPIP 90

7. Kinetic isotope effect parameters for the R67 DHFR and the wt. *E. coli* DHFR catalyzed reduction of DHB 90

8. Fluorometric parameters of R67 DHFR using FAD and FMN 91

9. Fluorometric parameters of R67 DHFR with PLP-AMP and Congo Red 91

10. Kinetic parameters for the R67 $DHFR_{double}$ catalyzed reduction of DHF..... 92

11. Fluorometric parameters for the R67 $DHFR_{double}$ binding NADPH 92

12. Kinetic isotope effect parameters for the R67 DHFR and the $DHFR_{double}$ catalyzed reduction of DHF 92

13. Kinetic parameters for the H62C R67 DHFR catalyzed reduction of acetyl-pyridine $NADP^+$ and NADPH.... 93

14. Kinetic parameters for the DHPR catalyzed reduction of MTHF 93

LIST OF ABBREVIATIONS

Å - Angstrom
α - Alpha
ß - Beta
ß-Me - ß-Mercaptoethanol
cm - Centimeter
°C - Degrees Celsius
Co. - Company
DCPIP - Dichlorophenolindophenol
DHB - 7,8-Dihydrobiopterin
DHF - dihydrofolate
DHFR - Native dihydrofolate reductase
DHPR - Dihydropteridine reductase
DNA - Deoxyribonucleic acid
E. coli - *Escherichia coli*
FAD - Flavin adenine dinucleotide
FMN - Flavin mononucleotide
FTHF - 10-Formyl-tetrahydrofolate
HCl - Hydrochloric acid
H62C R67 DHFR - site directed mutant of R67 DHFR in which the histidine at position 62 has been replaced with a cysteine
K. aerogenes - *Klebsiella aerogenes*
MET - 50 mM MES, 100 mM Tris-HCl, 50 mM Acetic acid buffer
MeTHF - Methenyl tetrahydrofolate
mM - micromolar
MTX - Methotrexate
μM - Micromolar
MTHF - Methylenetetrahydrofolate
MTHFD - Methenyl tetrahydrofolate dehydrogenase
MTHFR - Methylenetetrahydrofolate reductase
N - Normal

NAD^+ - Nicotinamide adenine dinucleotide oxidized form

NADH - Nicotinamide adenine dinucleotide reduced form

$NADP^+$ - Nicotinamide adenine dinucleotide phosphate oxidized form

NADPD - Deuterated nicotinamide adenine dinucleotide phosphate reduced form

NADPH - Nicotinamide adenine dinucleotide phosphate reduced form

NaOH - Sodium hydroxide

nm - nanometer

PLP-AMP - Pyridoxal-5'-disphospho-adenosine

q-DMP- quinonoid Dimethyl-dihydropterin

R67 $DHFR_{double}$- R67 DHFR protein which is encoded as a dimer

R-plasmids - Resistance plasmids

THF - tetrahydrofolate

THP - Tetrahydropterin

TMP - trimethoprim

UV/VIS - Ultraviolet/Visible spectrum

wt.- wild type

CHAPTER I

BACKGROUND

Dihydrofolate reductase (DHFR, EC 1.5.1.3) is a ubiquitous enzyme that plays a vital role in the metabolism of rapidly dividing cells. DHFR catalyzes the reduction of 7,8-dihydrofolate (DHF) to 5,6,7,8-tetrahydrofolate (THF) and uses the reduced form of nicotinamide adenine dinucleotide phosphate (NADPH) as a cofactor (Kraut, and Matthews, 1987). This enzyme allows a cell to maintain the intracellular pool of THF. This intracellular pool of THF is necessary for the production of some metabolic intermediates, such as purine nucleosides, and methionine. THF also acts as a coenzyme for the biosynthesis of thymidylate, and other metabolites which are necessary for the cell to function and grow normally (Blakley, 1969). If a cell's chromosomal DHFR is inhibited, the intracellular pool of THF will be reduced, the cell will then become unable to produce the metabolites needed to maintain life, and as a result the cell will die (Kraut, and Matthews, 1987).

Inhibition of chromosomal DHFRs has been used as a means of cancer therapy and also to combat microbial infections. From this work, several folate analogs have been synthesized for use as active site inhibitors of DHFR. For example, folate analogs such as trimethoprim (TMP), and methotrexate

(MTX), have been used in the treatment of cancer, malaria, microbial infections and several other diseases (Hitchings, 1983; Hitchings, and Baccanari, 1984). From the use of such active site inhibitors, the ease with which chromosomal DHFRs could be isolated and purified to homogeneity was simplified. This has lead to several bacterial and mammalian types of chromosomal DHFRs being, isolated, sequenced, and purified. From both DNA and protein sequence determinations, it is known that all chromosomal DHFRs are active as monomers which can have a molecular weight ranging from 18,000-22,000 daltons (Blakley, 1984).

In 1972, it was discovered that certain strains of *E. coli* and *K. aerogenes* had developed a significant tolerance to the antimicrobial agent TMP (Fleming *et al.* 1972). It was subsequently shown that the bacterial strain's tolerance was due to the presence of resistance plasmids (R-plasmids) which coded for novel DHFRs that have a reduced susceptibility to TMP (Amyes and Smith, 1974). These novel DHFRs were found to function at concentrations of TMP higher than that needed to completely inhibit the bacteria's chromosomal DHFR, and thereby protect the bacterial cells carrying these R-plasmids from the antibiotic TMP (Amyes and Gemmel, 1992). Since the initial discovery of R-plasmid DHFRs, there have been at least ten groups of R-plasmid DHFRs (designated types I-X) which have been isolated, identified and characterized for their biochemical and biophysical properties (Parrishall *et al.*,

1977; Jannsson, and Skold, 1991; Broad, and Smith, 1982; Young and Amyes, 1986; Joyner *et al.*, 1984).

The exact origin of R-plasmid encoded DHFRs is not well understood, however types I, III, IV, VI, and IX DHFRs have regions of their gene sequence which are homologous to the portion of the gene sequence which corresponds to the folate binding regions of the chromosomally encoded *E. coli* DHFR (Jannsson and Skold, 1991; Joyner *et al.*, 1984; Sundstrom, *et al.*, 1987; Thompson, Young and Amyes, 1990; Wylie and Koornhof, 1991). From these sequence studies, it has been suggested that type I, III, IV, VI, and IX DHFRs may have originated from the chromosomally encoded *E. coli* DHFR. The type II R-plasmid encoded DHFRs, however, show no sequence homology to any of the R-plasmid or chromosomally encoded DHFRs (Amyes and Gemmel, 1992). The type II R-plasmid encoded DHFRs are also structurally distinct from any of the chromosomally encoded DHFRs (Matthews *et al.*, 1986). It has been postulated that the type II R-plasmid encoded DHFR may have originated from some other bacterial oxidoreductase other than the chromosomally encoded DHFR (Stone and Smith, 1979). Another dissimilarity between type II R-plasmid encoded DHFRs and both the chromosomally encoded and the other types of R-plasmid encoded DHFRs, is that the type II R-plasmid DHFRs are the least susceptible to inhibition with TMP (K_i difference is approximately 10^6 (Amyes, 1989). This observation would also suggest that the type II R-plasmid DHFRs have a different and

unique origin from the chromosomally and other types of R-plasmid DHFRs.

Type II R-plasmid DHFR, of which three species have been characterized (R67, R388, and R751) (Broad and Smith, 1982), has shown to be functional as a tetramer. Sequence determinations between the three species show that there is greater than 75% homology between them (Amyes and Towner, 1990). The tetramer, which has been shown to possess a molecular weight of 34,000 daltons, consists of four identical monomers, each with a molecular weight of 8,300-8,500 daltons (Smith and Stone, 1979). Each monomer is encoded as a single 78 amino acid polypeptide. Monomers of R388 and R751 have been shown to be identical at positions 23 to 78. The R67 DHFR amino acid sequence when compared with R388 DHFR and R751 DHFR at positions 22-78 shows only six amino acid differences (Stone and Smith, 1979;, Flensburg and Steen, 1986; Swift, McCarthy and Heffron, 1981; Zolg and Hanggi, 1981). From these sequence determinations, type II R-plasmid DHFRs appear to contain a critical center domain which consists of residues 22-78. Further support for this hypothesis has been shown by Vermersch and Bennett (Vermersch and Bennett, 1986), and Reece *et al.* (Reece *et al.*, 1991). In experiments done by Vermersch and Bennett on R388 DHFR, removing the first 18 codons of R388 rendered the enzyme susceptible to TMP. However when 8 of the 18 codons were added back to the R388 TMP sensitive DHFR, the R388 DHFR again showed a high tolerance to TMP. Also, in the

experiments done by Reece *et al.* on R67 DHFR, when 16 N-terminal residues of the R67 DHFR were proteolytically cleaved it was found that the truncated R67 DHFR still retained full enzymatic activity. These results would support the hypothesis that type II R-plasmid DHFRs contain a critical center domain which consists of amino acid residues 22-78.

R67 DHFR, the focus of this research, and most of the research which is currently being performed on the type II R-plasmid encoded DHFR's, has been crystallized , both in its dimeric (Matthews *et al.* 1986) and tetrameric (Matthews, Xuong, Narayana, personal communication) forms. From these studies, it was found that the R67 DHFR does not possess any structural or sequence homology to the *E. coli* chromosomal DHFR. The crystal structure of the R67 DHFR dimeric form, shown in Figure 1 (all figures are contained within the Appendix) has been solved to a resolution of 2.8 Å and has a calculated R factor of 28 % for all data between 8 and 2.8 Å (Matthews *et al.* 1986). From the X-ray diffraction data, each of the R67 DHFR monomers has been shown to consist of an antiparallel ß-barrel with the fifth strand missing. The 18 amino-terminal amino acids are hydrophilic and form a completely disordered tail structure (Matthews *et al.* 1986).

The tetrameric crystal structure of R67 DHFR has been crystallized from an R67 DHFR variant enzyme with the first 16 amino-terminal amino acids missing (Reece *et al.* 1991). This crystal structure has been resolved to a resolution of 1.3 Å

with an R factor of less than 22 % for all data between 10 and 1.3 Å (Narayana, Xuong, and Matthews, personal communication). Tetrameric R67 DHFR, which is shown in figure 2, has a very unique attribute, a 24 Å long pore which passes through the center of the entire molecule with openings at both ends. Another interesting feature identified from the crystal structure is that each of the monomers crystallized identically and formed a tetramer with exact 222 symmetry.

Tetrameric R67 DHFR in ternary complex with NADPH and folate has also been crystallized (Matthews, Xuong, Narayana, personal communication). Unlike the chromosomal DHFR, the ternary complex containing the enzyme, NADPH and folate is inactive as the R67 DHFR does not have the ability to utilize folate as a substrate (Morrison and Sneddon, 1990). From difference density mapping it appears that the pterin ring of folate and the nicotinamide ring of NADPH stack adjacent to each other in the center of the pore. From this it could be postulated that all four monomers contribute to form a single active site.

The pH dependent kinetic parameters have been determined for R67 DHFR. Morrison and Sneddon have reported a half bell shaped pH profile for R67 DHFR which showed an ionization with a pKa of 6.4 for the plot of $V/Km_{(DHF)}$ and a pKa of 5.8 for the plot of V (Morrison and Sneddon, 1990) by using saturating (levels at 10 times the Kmat pH 7.0) levels of substrate and cofactor. A kinetic study done by Reece in 1990 showed half

bell shaped pH profiles of kcat and kcat/Km with an ionization pKa of 6.14 and 6.15 respectively (Reece-M.S. thesis). These studies (done by performing subsaturating kinetics) would indicate that R67 DHFR shows a titration in both the kcat and $kcat/Km_{(DHF)}$ profiles which corresponds to a group that titrates both in the enzyme-cofactor and the free enzyme complex (Fersht, 1985). Concurrently the pH behavior of the kinetic parameters exhibited by R67 DHFR with saturating NADPH would indicate that this ionization must be on the enzyme, because DHF does not exhibit a pKa near 6 (Morrison and Sneddon, 1990).

The most current mechanism for all chromosomal DHFR's maintains that the dihydropteridine ring of DHF must be protonated in order for hydride transfer from the cofactor, NADPH, to occur. In the proposed mechanism for the chromosomally encoded *E. coli* DHFR, proton delivery is believed to occur by way of an active site residue, Asp 27. The Asp 27 is thought to deliver a proton via an intermediate water molecule to the nitrogen at position 5 of the bound DHF. This would then facilitate hydride transfer from the C-4 carbon of NADPH to the C-6 carbon of the protonated ring of DHF (Stone and Morrison, 1988; Howell *et al.*, 1986).

From the determinations set forth for the chromosomally encoded *E. coli* DHFR it could be hypothesized that the R-plasmid DHFRs might have a similar reaction mechanism for the reduction of DHF to THF. From the observed kinetic pH

profiles it could be hypothesized that the active site pore of R67 DHFR should contain a residue with the ability to donate a proton which has a pKa of approximately 6, if the hypothesis the R-plasmid and chromosomally encoded DHFRs have similar reduction mechanisms. However, as previously discussed, from X-ray diffraction and crystallographic data, R67 DHFR contains a large pore in which the pteridine ring of DHF and the nicotinamide ring of the cofactor, NADPH, are stacked on top of one another in the center of the molecule, when the reaction takes place. Also from sequence comparisons of the active site pore of R67 DHFR and active site residues of *E. coli* DHFR, it was found that there isn't a potential proton donor in the R67 DHFR close enough to the pteridine ring of DHF to act in the same manner as the Asp 27 in the *E. coli* DHFR (Matthews *et al.*, 1986; Morrison and Sneddon, 1990). The observed kinetic pKa of the R67 DHFR (approximately 6) is now believed to be caused by protonation of the histidines which are located a positions 62, 162, 262, and 362 (as shown in Figure 2) (Matthews, Xuong, Narayana, personal communication; Nichols *et al.* 1992; Reece *et al.* 1990).

Currently the mechanism by which R67 DHFR performs the reduction of DHF to THF is not well understood; However a mechanism has been proposed which does take into account all data currently available. This mechanism, which is shown in Figure 3, proposes that the R67 DHFR binds a substrate which has been protonated in solution. Once the substrate has been

protonated, the hydride transfer from the N-5 position on the NADPH to the C-6 position of the pteridine ring of DHFR is able to take place and thus allow for the reduction of DHF to THF. This mechanism takes into account the structural data gathered for R67 DHFR such as: X-ray diffraction data which shows R67 DHFR to be a tetramer with the substrate and cofactor stacked adjacent to one another in the center of the active site pore of the molecule (Matthews, Xuong, Narraya, personal communication), a tetramer to two dimmer dissociation below pH 6 (Nichols, *et al.* 1992; Zhuang and Howell, 1993), and the observed kinetic data which show that the enzyme exhibits a marked decrease in activity below pH 6, and shows pKa of approximately 6 (Reece *et al.* 1990, Nichols *et al.* 1992). It would appear from the work done on the R67 DHFR that R67 DHFR did not originate from any of the chromosomally encoded DHFRs, but more possibly from another oxidoreductase (Smith and Stone, 1978).

Given R67 DHFR unique structure and symmetry of R67 DHFR, it is possible that R67 DHFR has the ability to utilize substrates with a similar structure to DHF. It will be the purpose of this thesis to explore the possibility that R67 DHFR has the ability to utilize different substrates. This study will examine kinetically and fluorometrically various pterin and folate structures as possible additional substrates which R67 DHFR has the ability to reduce, and also look into the possibility that R67 DHFR can bind cofactors other than

NADPH. Additionally, this thesis includes some kinetic studies which were performed on genetically altered R67 DHFRs for the purpose of comparison, both structurally and kinetically to the native R67 DHFR.

CHAPTER II

SUBSTRATE TOLERANCE STUDIES WITH R67 DHFR

INTRODUCTION:

7,8-Dihydrofolate (DHF), as previously discussed in Chapter I, is a known substrate for all DHFRs. The structure of 7,8-dihydrofolate, shown below, has a pteridine ring, with a 4-amino-benzoyl-glutamic acid tail (also shown below). DHFR converts DHF to THF, and thus allows a cell to maintain an intracellular pool of THF which a cell needs to survive and reproduce. R67 DHFR is known to reduce DHF and will be used in this thesis as means of ensuring the R67 DHFR protein is completely functional. R67 DHFR has been reported to utilize DHF at a rate of 1.3 sec^{-1}, with a Km_{DHF} of 5.8 μM, and NADPH K_m of 3.0 μM. (Reece, thesis).

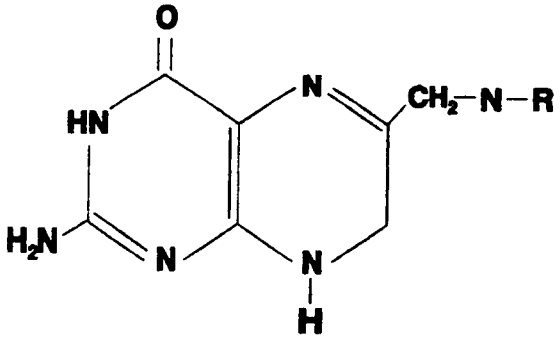

Structure of Dihydrofolate
Blakely, 1969

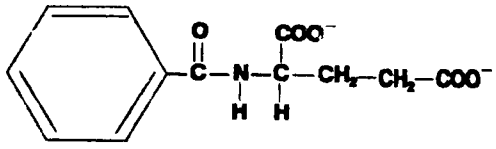

4-amino-benzoyl-glutamic
acid tail structure of DHF

It will be the purpose of this chapter to investigate R67 DHFRs ability to utilize substrates which are similar in structure to DHF. The substrates tested were: quinonoid-6,6-dimethyl-dihydropterin tautomer (q-DMP), methylenetetrahydrofolate (MTHF), 7,8-dihydrobiopterin (DHB), dichlorophenolindophenol (DCPIP), methenyltetrahydrofolate (MeTHF), 10-formyltetrahydrofolate (FTHF), sepiapterin, and uracil. Below is a description of each of the substrates tested and their importance in the cell.

q-DMP:

q-DMP is a known substrate for the enzyme dihydropteridine reductase (DHPR). The structure of this q-DMP tautomer, shown below, possesses a very similar structure to that of DHF, a known substrate for R67 DHFR. Structural differences occur in the tail structure of both compounds.

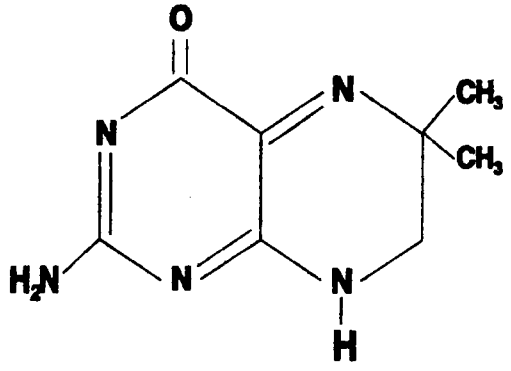

Structure of q-Dimethyldihydropterin tautomer, Armarego *et al.*, 1989

DHPR was initially isolated from rat liver tissue (Craine *et al.* 1972), and functions in keeping a fully reduced pool of tetrahydropterin (THP) and/or tetrahydrobiopterin. THP is needed for the synthesis of important amino acids such as tyrosine (schematic diagram of THP regeneration is shown in Figure 4), and is used as a cofactor for the aromatic amino acid hydroxylases which produce DOPA, 5-hydroxytryptophan and enzymes which cleave glyceryl ethers to glycerol and fatty aldehydes (Smith and Nichol, 1986; Kaufman and Fisher, 1974).

DHPR is an NADH-dependent reductase which is known to be able to utilize the quinonoid form of both dihydropterin and dihydrobiopterin (Craine, *et. al.* 1972). Several studies have shown the quinonoid form of both compounds to be highly unstable and spontaneously form the 7,8-dihydropterin or 7,8-dihydrobiopterin tautomer respectively, which have been shown not to be utilized by DHPR (Amarego, *et. al.* 1983; Ayling, *et. al.* 1989; Armarego, 1989). Due to this unstablility of the natural substrate tautomer, several studies have been conducted to generate a "stable" q-dihydropterin tautomer so that accurate kinetic measurements could be obtained (Bailey and Ayling, 1983). In a study done by Ayling, a "stable" q-dihydropterin tautomer, q-6,6-dimethyldihydropterin, was generated and shown to be stable for approximately 15-20 minutes when the solution was kept under a vacuum (Bailey and Ayling, 1983). From using the q-DMP as a substrate for DHPR (purified to homogeneity from the sheep liver), it was found

that the k_{cat} of the reaction is approximately 2.2 sec^{-1}, and has K_m for NADH of 5.7 μM, and a K_m for q-DMP of 15.2 μM (Craine, et al. 1972). Also DHPR has been shown to utilize NADH better than NADPH (Craine, *et al.* 1972; Nielsen *et al.* 1969).

The crystal structure for the rat liver DHPR has been solved (Matthews, *et al.*, 1991). The DHPR crystal structure (Figure 5) shows that the protein is functional as a dimer with a molecular weight ranging from 41,000 to 42,800 daltons. From the diffraction data which have been gathered the DHPR crystal structure does not show a proton donor in or near the active site with the possible exception of a tyrosine (Matthews *et al.* 1992).

MTHF:

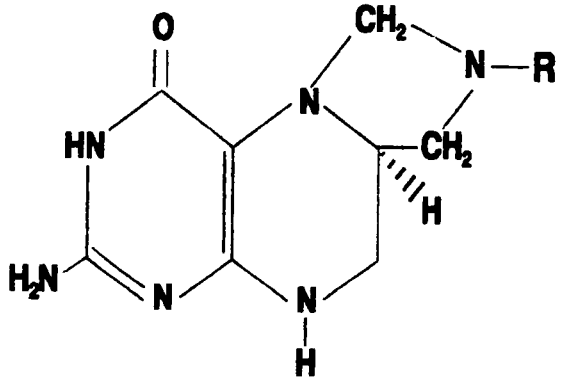

structure of
Methylenetetrahydrofolate
Matthews, 1986

MTHF is a known substrate for the enzyme Methylenetetrahydrofolate Reductase (MTHFR). The structure shown above has

the same basic pteridine ring structure as that of DHF. The dissimilarity between DHF and MTHF is found at the nitrogen 5 position of MTHF. At this position MTHF shows an exocyclic ring structure.

MTHFR, first isolated from pig liver, is a flavoprotein which contains FAD as a noncovalently bound cofactor (Donaldson, and Keresztesy, 1962; Kutzbach, and Stakstad, 1971; Matthews and Kaufman, 1967). MTHFR catalyzes an NADPH dependent reduction of MTHF to 5-methyl-tetrahydrofolate (Matthew, and Haywood, 1979). MTHFR is necessary for the synthesis of dTMP, and purine biosynthesis. Inhibition of MTHFR will result in the loss of available 5-methyl-tetrahydrofolate and ultimately in the shutdown of the thymidylate synthetase pathway and some of the S-adensoylmethionine-dependent methylation reactions.

The proposed mechanism for MTHFR, found in figure 6, shows that the MTHF undergoes an acid catalyzed ring opening to form a 5-iminium cation which then tautomerizes to form a quinoniod 5-methyldihydrofolate. It is believed that the quinoniod 5-methyldihydrofolate is then reduced to the 5-methyltetrahydrofolate (Matthews, and Kaufman, 1980; Matthews, and Haywood, 1979). From kinetic studies using NADPH, it has been found that MTHFR can reduce MTHF at a rate of 0.86 sec^{-1}, and has K_m values of 20 μM and 16 μM, for the MTHF and NADPH, respectively.

It has also been shown that MTHFR can support

phenylalanine hydroxylation by the regeneration of THP. In this study (Matthews and Kaufman, 1980) we have found that MTHFR possessed the ability to catalyze the reduction of q-DMP. The kinetic parameters which were generated showed a V_{max} of 0.08 sec^{-1} (Matthew and Kaufman, 1980).

DHB:

DHB is the spontaneous degradation product of quinonoid-dihydrobiopterin. DHB is similar in structure to DHF. The dissimilarity between DHB (shown below) and DHF can be found in the tail structure of the DHB which is a isopropylalchol, whereas the tail structure of DHF consists of a 4-amino-benzoyl-glutamic acid (shown on page 11).

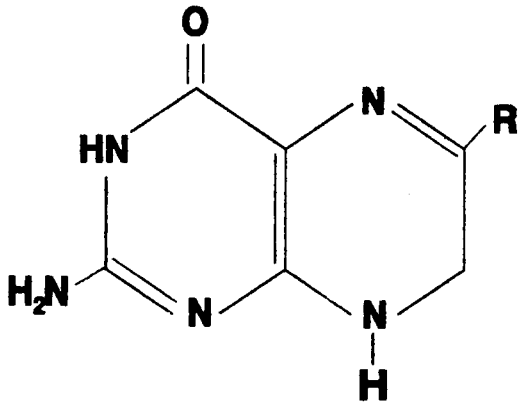

Structure of
7,8-Dihydrobiopterin
Blakley, 1961

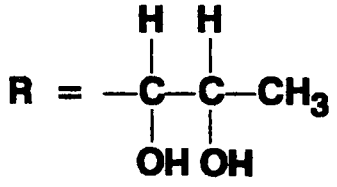

Structure of DHB's
R-group

DHB is the oxidized form of tetrahydrobiopterin (THB). THB as mentioned in the previous section, is used by phenylalanine-4-monooxygenase, which is involved in the

degradation of phenylalanine to tyrosine (Smith and Nichol, 1986). Figure 4 show the pathways in which THP is maintained. From the figure, we can see that there are two main routes which are elicited in the recycling of THB, one through a reduction reaction of quinonoid-THB with the use of DHPR, and a second pathway in which DHB is converted to THB through the use of wt. *E. coli* chromosomal DHFR.

DCPIP:

DCPIP, structure shown below, is a commercial dye which has been used in assaying for diaphorase activity. Diaphorase activity is the general term given to groups of enzymes which have the ability to reduce dyes such as Nitro blue tetrazolium and DCPIP.

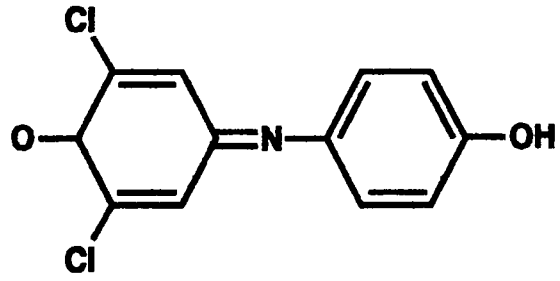

Structure of
Dichlorophenolindophenol
Merck Index, 244

MeTHF:

MeTHF, shown below, differs from THF at positions N5 and N10. At these positions we can see that an exocyclic ring structure between the two nitrogens has been formed. MeTHF is

the substrate for methenyltetrahydrofolate dehydrogenase. This enzyme takes the MeTHF and converts it to MTHF with the aid of $NADP^+$. In the FTHF (shown below), interconvertable with MeTHF with the help of cyclohydrolase (Zubay, 1988), a difference is observed compared to THF at the N10 position. At this position of FTHF we can see an addition of a formyl group.

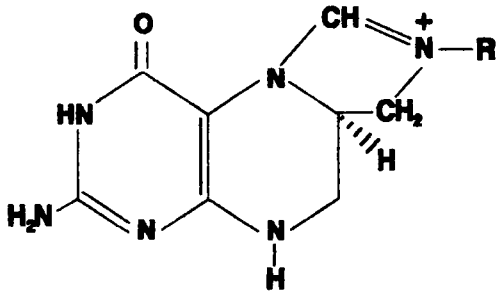

Structure of MeTHF
Zubay, 1988

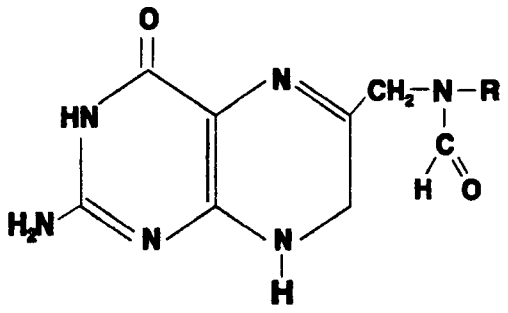

Structure of FTHF
Zubay, 1988

Sepiapterin:

Sepiapterin,or 6-lactoyl-7,8-dihydrobiopterin (shown below), is the precursor of DHB. Sepiapterin differs from DHB (shown on page 16) in the structure of the tail region.

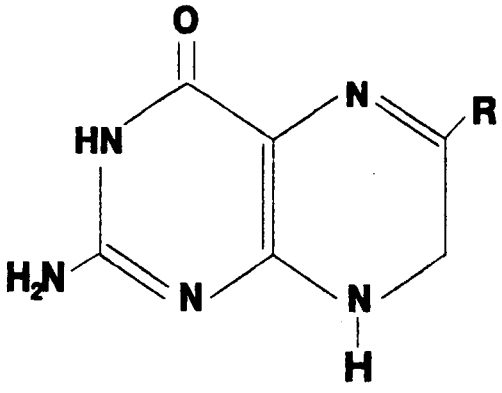

Structure of Sepiapterin
Blakley, 1961

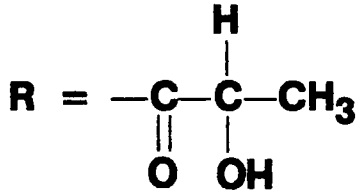

Structure of the R-group of
Sepiapterin Blakley, 1961

Uracil:

Uracil, shown below, which is used in a dihydropyrimidine reduction reaction, was also used as a possible compound which might also be able to be utilized by R67 DHFR in a reduction reaction.

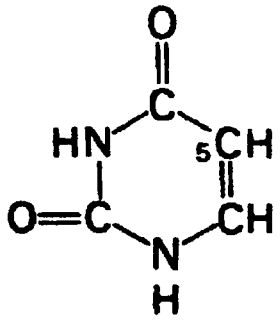

Structure of Uracil
Zubay, 1988

METHODS AND MATERIALS:

R67 DHFR PROTEIN PURIFICATION:

The R67 DHFR protein was expressed and purified as previously described by Reece *et al.*, 1990. Briefly, the *E.coli* strain SK388 with a cloned R67 DHFR gene (P700), which was a generous gift from L. Elwell at Burroughs Research Laboratories (Research Triangle Park, NC.), was grown in TB media to the stationary phase. The cells are lysed with addition of 2N NaOH until a pH of 12 is reached. The solution is centrifuged and the pH of the supernatant is then lowered to a pH of 2. The solution is then centrifuged and the

remaining supernatant is then adjusted to a pH of 7.0, and dialyzed against 25 mM imidazole buffer (Sigma Chemical Co.), with a pH of 7.4. The equilibrated solution is then loaded onto a 1.0 cm X 30 cm PBE chromatographic focusing column (Pharmacia), and the protein is eluted with a 1:8 dilution of Polybuffer 74 (Pharmacia), pH 4.0. The fractions which contained R67 DHFR were collected, pooled, and then passed over a 2.5 cm X 90 cm G-75 Sephadex column. The fractions which contained R67 DHFR were concentrated, dialyzed against distilled water, lyophilized and stored at 4°C until use.

KINETIC ASSAYS:

PREPARATION AND STABILIZATION OF SUBSTRATES:

DHF:

DHF was prepared by C.Linn for our laboratory using the method of R.L. Blakley, 1961. Briefly, folic acid is resuspended in 1N NaOH. A 50 mM ascorbic acid solution is added to the folic acid and solution is mixed. To the folic/ascorbic acid solution, sodium dithionite is added and allowed to stir for 5 minutes. After incubation the solution is cooled to 5 °C and 1N HCl is added until the pH of the solution reaches 2.8. At this point the DHF precipitates. The solution is centrifuged and the pellet is resuspended in ascorbic acid solution. To this solution 1N NaOH is added until a pH of 6.0 is reached. At this point 1N HCl is added

until a pH of 2.8 is achieved and at which point the DHF will crystallize out of solution. The solution is centrifuged and the DHF pellet is washed, and resuspended in 0.005 N HCl, centrifuged and the pellet resuspended in 0.005 N HCl and 50 μM ß-Mercaptoethanol (ß-Me). The solutions were kept at -70°C, until use.

Q-DMP:

6,6-Dimethyl-5,6,7,8-tetrahydropterin and NADH were purchased from Sigma Chemical Co.. The 6,6-Dimethyl-5,6,7,8-tetrahydropterin was used to generate the substrate, q-DMP. The generation of the q-DMP must be done prior to each kinetic measurement as the q-DMP is unstable in the presence of oxygen. Generation of q-DMP involves the addition of peroxide and peroxidase to the solution of 6,6-Dimethyl-5,6,7,8-tetrahydropterin and incubating the mixture for 2 minutes. Figure 7 shows a UV/VIS spectrum of the 6,6-Dimethyl-5,6,7,8-tetrahydropterin before (figure 7A) and after the addition and incubation with peroxide and peroxidase (figure 7B). In this figure it can be seen that there is an appearance of an additional peak in the UV/VIS spectrum of the 6,6-Dimethyl-5,6,7,8-tetrahydropterin after its incubation with peroxide and peroxidase, corresponding to the formation of q-DMP.

MTHF:

MTHF was purchased from Dr. B. Schircks Laboratories

(Switzerland). MTHF is known to be unstable in the presence of oxygen and is also light sensitive (Matthews, and Haywood, 1986). Therefore the substrate was dissolved in MET buffer (pH 7.00) into an epitube which was maintained in a constant nitrogen environment and also protected from light. MTHF concentrations were determined by measuring the absorbance (anaerobically) at 297 nm using an extinction coefficient of 32 μM^{-1} cm^{-1} (Blakley, 1969). To ensure MTHF was not being degraded by oxygen in between kinetic measurements, UV/VIS spectra were performed at five minute intervals between kinetic measurements (see figure 8 for sample spectra).

DHB:

DHB used in this section was purchased at Dr. B. Schircks Laboratories (Switzerland). DHB has an absorbance maximum of 340 nm and a molar extinction coefficient of 11,920 $cm^{-1}M^{-1}$ and is known to be stable in the presence of oxygen and is not light sensitive, and stock solution of DHB were maintained in a 1M Tris buffer pH 7.0 until use.

DCPIP:

DCPIP was purchased from Sigma Chemical Co.. DCPIP is stable in the presence of oxygen, but is light sensitive, therefore the stock solutions of DCPIP were kept on ice and protected from light until assay was begun. DCPIP was

resuspended in a MET buffer at pH 7.0 which did not contain ß-Me (which would increase the nonenzymatic degradation of the substrate). DCPIP concentrations were determined by measuring the absorbance at 515 nm using an extinction coefficient of 15.2 μM^{-1} cm^{-1}.

MeTHF:

MeTHF was purchased from Dr. B. Schircks Laboratories (Switzerland). MeTHF has an absorbance maximum at 293 nm and is both oxygen and light sensitive. The MeTHF stock solution was maintained under nitrogen and protected from light, and absorbance scans of the solution were taken at approximately five minute intervals to ensure that the substrate was not being degraded. Figure 9 shows two sample scans which were taken.

FTHF:

FTHF was purchased from Dr. B. Schircks Laboratories (Switzerland). FTHF was generated fresh each day, by allowing MeTHF to stand in the presence of 0.1 M Tris pH 8.0 with 0.01 M ß-Me for three hours at 25 °C in the presence of nitrogen, and protected from light. Figure 10 shows scans which were taken before and after the FTHF was generated. These scans show that, after incubation of the MeTHF with 0.1 M Tris pH 8.0 and 0.01 M ß-Me, there is the emergence of a new peak at approximately 250 nm which corresponds to the formation of

FTHF.

FTHF has an absorbance maximum of 258 nm and a molar extinction coefficient of 22,310 cm^{-1} M^{-1}. FTHF dehydrogenase catalyzes the reaction FTHF + $NADP^+$ --->THF + NADPH and is irreversible with the pig liver enzyme. The FTHF stock solution (maintained in a MET buffer with ß-Me, at pH 8.0 under nitrogen) was monitored by absorbance scans at approximately five minute intervals to ensure that the substrate was not degraded. Figure 10 shows two sample scans of the FTHF solution which were taken.

Sepiapterin:

Sepiapterin was purchased from Dr. B. Schircks Laboratories (Switzerland). Sepiapterin, plays a role in the biosynthesis of tetrahydrobiopterin. Sepiapterin reductase catalyzes the formation of dihydrobiopterin from sepiapterin and requires NADPH as a cofactor. Sepiapterin has an absorbance maximum at 420 nm and a molar extinction coefficient of 10,400 cm^{-1} M^{-1}. Sepiapterin is known to be unstable in the presence of oxygen and is slightly light sensitive. The sepiapterin stock solution was maintained under nitrogen, and absorbance scans (shown in figure 11) were run on the substrate at approximately five minute intervals to ensure that the substrate was not degraded.

Uracil:

Uracil and 5-fluoro-uracil were purchased from Sigma Chemical Co.. Uracil is known to be stable, so no special precautions were taken to stabilize the substrate.

NADPD PREPARATION AND PURIFICATION:

NADPD was prepared from $NADP^+$ by the method of Viola, 1984. Briefly, 75 mg of $NADP^+$ was dissolved in 5 mls of 6 mM N-tris(hydroxymethyl)methyl-3-amino propanesulfonic acid (TAPS) buffer pH 9.0. 6 μl of deuterated ethanol, 100 μl aldehyde dehydrogenase solution and 2 mg of alcohol dehydrogenase are added to the $NADP^+$ solution. The solution is stirred and maintained at a pH of 9.0 with additions of 0.1 M potassium hydroxide while checking the absorbance of the solution at 340 nm until the absorbance ceases to increase. The solution is filtered using a YM10 filter to remove enzymes, the filtrate is scanned from 200 nm to 400 nm, and the 260/340 ratio is calculated (NADPD, has an absorbance maximum at 340, the smaller the 260/340 ratio is, the less unconverted $NADP^+$, which has an absorbance maximum at 260, is in the solution). The resulting NADPD is separated from the unreacted $NADP^+$ by loading the solution on to a DEAE fractogel column equilibrated in 10 mM Imidazole pH 7.5 with a flow rate of 0.25ml/min. The NADPD is eluted with a 0 - 0.4 M potassium chloride (pH 7.5) gradient, and fractions with a lower 260/340 ratio are pooled and loaded onto a P2 column using a flow rate

of 0.2ml/min and collected in 2 ml fractions. Fractions are then selected on the basis of 260/340 ratio and a negative reaction to silver nitrate. The resulting solutions are pooled and lyophilized.

KINETIC MEASUREMENTS:

Michaelis-Menten kinetics were attempted with all of the substrates previously mentioned. The kinetic rates were determined spectrophotometrically using a Perkin Elmer UV/VIS Lambda 3B spectrophotometer. After the addition of substrate and cofactor the assay was initiated by the addition of enzyme and the initial rates of reaction were measured spectrophotometrically using the computer program UVS (Softways) by measuring the loss in absorbance at 340 mM, which corresponds to the loss of reduced cofactor, at 30 °C for one minute. All compounds (see table 1 for the pKas and extinction coefficients of compounds tested) were dissolved in a polybuffer consisting of 100 mM Tris-HCL, 50 MES, 50 mM Acetic acid, 10 mM ß-Me (pH 7.0), and maintained on ice throughout the assay period. The rate of non enzymatic degradation of substrate and cofactor was subtracted out by using a second cuvette containing only substrate and cofactor. For each of the substrates tested with R67 DHFR a similar experiment involving the chromosomal *E. coli* DHFR was also performed. These resulting data were then fit to the Michaelis-Menten equation using non-linear regression program,

EnzFitter (Elsevier-Biosoft). Some of the substrates utilized in this chapter required slight deviations from the above procedure, therefore a brief description of the methods employed with these substrates is described below:

MTHF, MeTHF, AND FTHF:

After ensuring that the substrates were stable, kinetic measurements were done using NADPH or $NADP^+$, and R67 DHFR. Kinetic determinations were done anaerobically using Thunberg cuvettes. After the addition of MET buffer, pH 7.00, the cuvettes were then bubbled with nitrogen and sealed. All additions made to the cuvettes after this point are made using Hamilton gas-tight syringes or a pipetman equipped with a syringe needle.

DCPIP:

As mentioned previously, DCPIP is a commercially available dye which can be spontaneously reduced by NADPH, therefore this set of subsaturating kinetics were performed in a buffer that was devoid of the 10 mM ß-Me which is normally found in MET buffer.

RESULTS AND DISCUSSION:

The data generated from the substrate tolerance studies on R67 DHFR are shown in figures 12-16. Table 2 shows the kinetic data which were gained from the replots of the primary

data for DHF. Briefly, the K_m for DHF was 6.9 μM, the K_m for NADPH was 3.1 μM, and these data sets showed a k_{cat} of 1.2 sec^{-1}. From these results, it is clear that the k_{cat} and K_m values for the R67 DHFR catalyzed reduction of DHF to THF are easily reproducible. In a recent study done by Reece *et al.* 1990, the K_m for DHF was 5.8 μM and the K_m for NADPH was 3.0 μM. The values generated in this study show K_m's for both substrates are comparable and within error limits. The k_{cat} in the study done by Reece *et al.* 1990, showed a k_{cat} of 1.3 sec^{-1} which is also comparable to the k_{cat} of 1.2 sec^{-1}.

From the replots of the kinetic data gathered for q-DMP, MTHF, DHB and DCPIP we have shown that all of these compounds can be utilized by R67 DHFR in a reduction reaction. Tables 3-6 show the k_{cat} and K_m values which were generated from the replots of the original data for q-DMP, MTHF, DHB and DCPIP. The k_{cat} and K_m values generated from these substrates are: for q-DMP a k_{cat} of 0.4 sec^{-1}, $K_{m(NADPH)}$ 11 μM, and a $K_{m(q\text{-}DMP)}$ of 185 μM; for MTHF a k_{cat} of 0.8 sec^{-1}, $K_{m(NADPH)}$ 7.1 μM, and a $K_{m(MTHF)}$ of 78.1 μM; for DHB a k_{cat} of 0.9 sec^{-1}, $K_{m(NADPH)}$ 7.2 μM, and a $K_{m(DHB)}$ of 20.8 μM; for DCPIP a k_{cat} of 0.4 sec^{-1}, $K_{m(NADPH)}$ 5.3 μM, and a $K_{m(DCPIP)}$ of 32.9 μM. These substrates have also been tested both with their native enzymes and with the chromosomal *E. coli* DHFR (Data generated from these experiments are also found in tables 3-6). The results of these substrates being utilized by their native enzymes, show that the methods used for assaying activity are valid, and would suggest that the

K_ms and k_{cat}s calculated for the R67 DHFR catalyzed reductions in this chapter are real, and not due to the spontaneous reduction of substrate in solution. These results also show that, of the substrates tested, DHB, was the only substrate able to be utilized by *E. coli* DHFR. This result is probably due to the very similar structure of DHB and DHF.

Since both R67 DHFR and chromosomal *E. coli* DHFR have the ability to utilize DHB as a substrate in a reduction reaction, the question was asked whether the rate determining step of both the R67 DHFR and *E. coli* chromosomal DHFR's reactions are directly comparable. To this end we performed NADPD isotope effect studies on both enzymes. The data generated from this study are shown in figure 17. From these data both k_{cat} values (shown in table 7) for NADPH and NADPD can be generated for both R67 DHFR and *E. coli* chromosomal DHFR. By comparing the NADPD vs. NADPH k_{cat}s of the enzymes ^{D}V values may be generated. R67 DHFR showed a k_{cat} using NADPH of 0.89 sec^{-1} and a k_{cat} using NADPD of 0.24 sec^{-1}. *E. coli* chromosomal DHFR showed a k_{cat} using NADPH of 2.13 sec^{-1} and a k_{cat} using NADPD of 1.06 sec^{-1}. From the k_{cat}s which were determined, the ^{D}V value for substitution of NADPD for NADPH in R67 DHFR is 3.71, and the ^{D}V value in E. coli chromosomal DHFR is 2.26. From this experiment, it would appear that the rates of catalysis of DHB are not truly comparable, as the *E. coli* chromosomal DHFR catalyzed reduction does not shown the same isotope effect that the R67 DHFR shows. R67 DHFR's isotope effect shows that

the rate determining step of the reaction is hydride transfer whereas *E. coli* DHFR's isotope effect shows that hydride transfer is only partially rate limiting.

From this study we have also shown that R67 DHFR and chromosomal *E. coli* DHFR are unable to utilize MeTHF, FTHF, sepiapterin, uracil, and 5-fluoro-uracil.

This study has investigated R67 DHFRs substrate tolerance limits. We have shown R67 DHFR to possess a greater range of substrate utilization than its chromosomal counterpart *E. coli* DHFR. R67 DHFR has the ability to utilize DHF, q-DMP, MTHF, DHB, and DCPIP. The chromosomal *E. coli* DHFR has been shown to be able only to utilize DHF and DHB.

Investigation of substrate pKas from the substrate which can be utilized by R67 DHFR may aid in furthering the proposed mechanism of R67 DHFR (mechanism is shown in figure 3). R67 DHFR catalyzed reduction has been proposed to be dependent on binding substrate which has been protonated in solution and not by an active site residue (as is the case with the chromosomal *E. coli* DHFR). Folate is a substrate for chromosomal *E. coli* DHFR, but it is not a substrate for R67 DHFR. The pKa for folate is approximately -1.8 . It is generally believed that folate is not a substrate for R67 DHFR because of its pKa, which would suggest that at pH 7.0 virtually none of the folate in solution would be protonated. On the other hand the substrates which have been shown in this study to be utilized by R67 DHFR have pKas which are

obtainable (see table 1) and allow for some of the substrate to exist as a protonated species in solution. This protonated species would be the activated substrate which could be used by R67 DHFR.

CHAPTER III

VARIANT LIGAND BINDING STUDIES WITH R67 DHFR

INTRODUCTION:

DHFRs require a nicotinamide cofactor to reduce DHF to THF. *E. coli* chromosomal DHFR utilizes both ß-NADPH and ß-NADH as cofactors in the reduction reaction, but the *E. coli* enzyme cannot utilize the α forms of either NADPH or NADH. In contrast, R67 DHFR can utilize both the α and ß forms of NADPH. This would suggest that R67 DHFR and *E. coli* chromosomal DHFR bind cofactor differently.

It is the purpose of this section to investigate whether R67 DHFR possesses the ability to bind cofactors which possess a similar function to the nicotinamide cofactors. This section investigates the possibility that R67 DHFR has an ability to bind flavin adenine dinucleotide (FAD), flavin mononucleotide (FMN), pyridoxal 5'-diphospo-5'adenosine (PLP-AMP), and congo red, a diazo series acid dye. Below is a brief description of all variant cofactors tested.

FAD and FMN (shown on the next page) are the two active coenzyme forms of riboflavin (vitamin B_2) (Zubay, 1988).

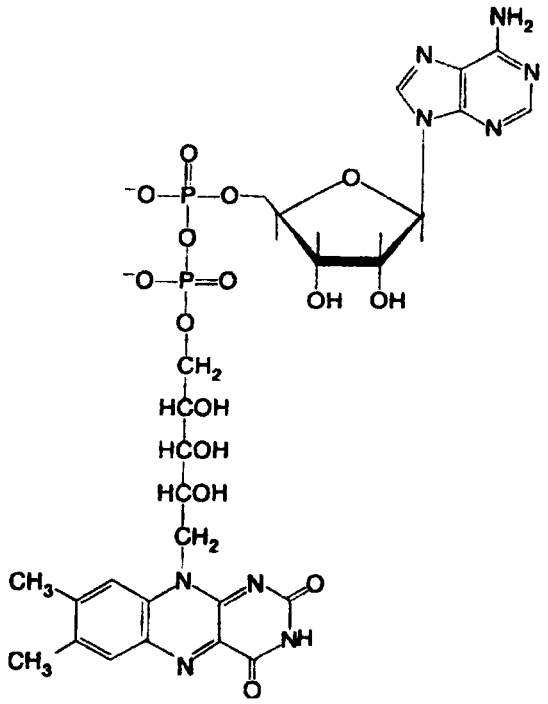

Structure of Flavin Adenine Dinucleotide, Zubay, 1988

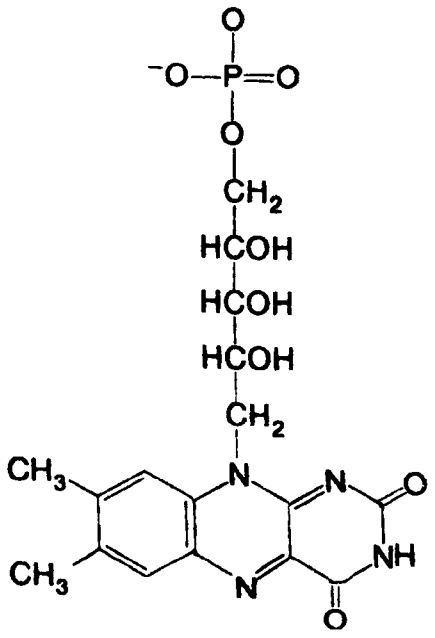

Structure of FMN Zubay, 1988

Pyridoxal 5'-diphosho-5'adenosine (PLP-AMP), shown below, has been used in a number of nucleotide-binding enzymes as an affinity probe (Tamura, Rakov, and Cross, 1986). PLP-AMP is similar in structure to the known cofactor, NADPH for R67 DHFR.

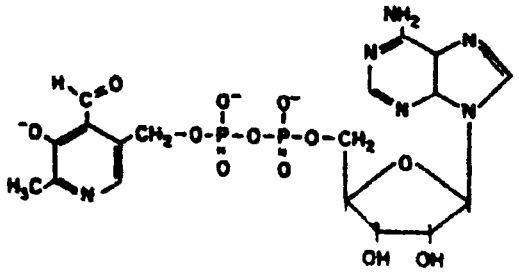

Structure of PLP-AMP
Tamaura, Rakov, and Cross, 1986

Congo Red (shown below) is an acid dye from the diazo series (Gurr, 1960). The molecule consists of two identical halves. Each half of congo red is composed of a phenyl ring which is linked to naphthalene by a diazo group (Turnell and Finch, 1991). Congo red has been used to detect the presence of amyloid plaques and has been found to bind to proteins whose structure consists mainly of ß-sheet (Castano and Frangione, 1988).

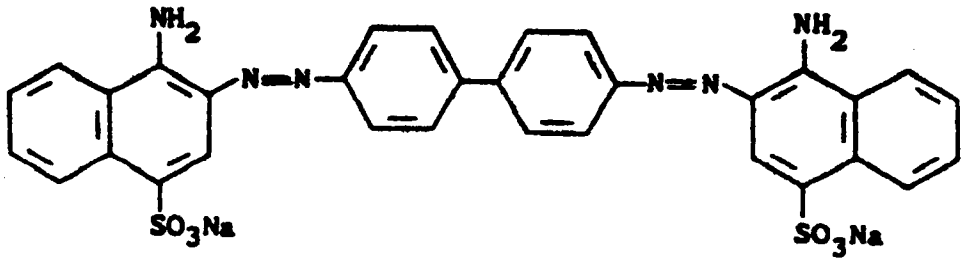

Structure of Congo Red
Turnell and Finch, 1991

METHODS AND MATERIALS:

FLUOROMETRIC MEASUREMENTS:

FAD:

FAD which was purchased from Sigma Chemical Co., has an extinction coefficient at 450 nm of 11.3 μM^{-1} cm^{-1}. FAD in concentrations of 40 - 400 μM was resuspended in MET buffer pH 7.0 and added in small aliquots to 6 μM R67 DHFR protein. The

intrinsic protein fluorescence was monitored at 25 °C using a Perkin-Elmer LS-5B spectrometer.

The fluorescence of 6 μM R67 DHFR at pH 7.0 was quenched by the addition of small aliquots of FAD. Trytophans (tetrameric R67 DHFR contains eight tryptophan residues) were excited at 290 nm and the fluorescence emission was monitored at 340 nm. Quenching of a D, L-tryptophan control was also performed using identical conditions.

A second set of fluorescence experiments, using R67 DHFR and FAD, were also performed as described above with the exception that the excitation and emission wavelengths were changed from 290 and 340 to 450 and 527, respectively. This change in the excitation and emission wavelength allows for the measurement of fluorescence of the FAD.

FMN:

FMN was purchased from Sigma Chemical Co.. FMN (extinction coefficient at 450 nm of 11.3 μM^{-1} cm^{-1}) in concentrations of 40 - 400 μM was resuspended in MET buffer pH 7.0 and added in small aliquots to 5 μM R67 DHFR protein. The intrinsic protein fluorescence was monitored at 25 °C using a Perkin-Elmer LS-5B spectrometer.

The fluorescence of the 5 μM R67 DHFR at pH 7.0 was quenched by the addition of small aliquots of FMN. Trytophans were excited at 290 nm and the fluorescence emission was monitored at 340 nm. Quenching of a D, L-tryptophan control

was also performed using identical conditions.

A second set of fluorescence experiments, using R67 DHFR and FMN, were also performed as described above with the exception that the excitation and emission wavelengths were changed from 290 and 340 to 366 and 527, respectively. This change in the excitation and emission wavelength allows for the measurement of FMN fluorescence.

PLP-AMP and congo red:

PLP-AMP was a generous gift from Dr. E. Serpersu, and the congo red was purchased from Sigma Chemical Co. PLP-AMP or congo red in concentrations of 40 - 400 μM was resuspended in MET buffer pH 7.0 and added in small aliquots to 3 μM R67 DHFR protein. The intrinsic protein fluorescence was monitored at 25 $^{\circ}$C using a Perkin-Elmer LS-5B spectrometer.

The fluorescence of the 3 μM R67 DHFR at pH 7.0 was quenched by the addition of small aliquots of PLP-AMP or Congo red. Trytophans were excited at 290 nm and the fluorescence emission was monitored at 340 nm. Quenching of a D, L-tryptophan control was also performed using identical conditions.

PLP-AMP also has the ability to form a Schiffs base with lysine. This formation causes a change in the absorbance of the PLP-AMP. Since R67 DHFR contains a number of lysine residues, absorbance spectra of the PLP-AMP before and after the addition of protein to the sample were taken. Figure 18,

shows the before and after scans of the PLP-AMP. These scans do not show any appreciable difference that would suggest that the PLP-AMP is forming a Schiffs base with any of the lysine residues from the protein.

DATA ANALYSIS:

Data generated from the 290/340 tryptophan fluorescence quenching experiments were analyzed by Statistical Analysis Software (SAS) using the equation:

$$Y=100-0.5\ F_o\ (R_o + Kd + L_{tot}) - [(R_o + Kd + L_{tot})^2 - 4.0\ R_o\ L_{tot}]^{1/2}$$

Data generated from the second set of fluorescence experiments with both FAD and FMN were also analyzed in SAS using the equation:

$$Y=\ 0.5\ F_o\ (R_o + Kd + L_{tot}) - [(R_o + Kd + L_{tot})^2 - 4.0\ R_o\ L_{tot}]^{1/2}$$

In both cases, 100 represents the initial fluorescence maximum (without ligand present) converted to 100 percent, F_o represents the observed fluorescence converted to a percent by dividing by the initial fluorescence, R_o represents the total enzyme concentration multiplied by the n (known as the stoichiometry of binding), L_{tot} represents the total ligand concentration, Kd represents the dissociation constant, and Y represents the normalized fluorescence.

RESULTS AND DISCUSSION:

The data generated from performing the variant cofactor binding studies with R67 DHFR, using FAD, FMN, PLP-AMP, and congo red are shown in figures 19-24. These figures represent the percent fluorescence vs. the ligand concentration. From these plots the binding stoichiometry and Kd can be identified.

Table 8 shows the values which were obtained from fitting of the data for both FAD and FMN. Briefly, the data for the 290/340 and 450/540 excitation/emission of R67 DHFR with FAD show binding stoichiometries of 0.34, 0.37 and Kd values of 1.5 μM, 1.6 μM, respectively. The data from the 290/340 and 366/527 excitation/emission of R67 DHFR with FMN shows binding stoichiometry of 3.3, 3.7 and Kd values of 3.3 μM, and 3.5 μM, respectively.

Table 9 shows the values which were generated from the from the tryptophan fluorescence quenching experiments performed on R67 DHFR using PLP-AMP and congo red. The data show that PLP-AMP and congo red have the ability to bind to R67 DHFR with binding stoichiometries of 5.1 and 1.3 and Kd values of 65 μM and 246 μM, respectively.

From the results shown in tables 8 and 9, we have shown R67 DHFR to be able to bind the flavin cofactors FAD, and FMN, the affinity probe PLP-AMP, and the dye congo red . From concurrent fluorescence quenching studies with *E. coli* chromosomal DHFR using FAD, FMN, and PLP-AMP, we have also

shown that *E. coli* chromosomal DHFR does not possess the ability to bind any of the compounds tested. These results would suggest that R67 DHFR binds cofactors differently than its chromosomal counterpart. These results might also suggest that R67 DHFR originated from an oxidoreductase different than chromosomal DHFRs, or that the R67 DHFR active site pore is just a hydrophobic pocket which has not been specialized.

Although it seems unusual that the binding stoichiometries of FAD to R67 DHFR are low (ratios of approximately 1:3), while the binding stoichiometries measured for FMN, are higher (ratios of approximately 4:1), both sets of data sets agree (fall within one standard deviation), and are reproducible. Another result which must also be considered when looking at these ratios of bound ligand to R67 DHFR is that the known substrate for R67 DHFR, DHF, when used as a quencher in tryptophan fluorescence quenching experiments does not show a 1:1 ratio of ligand to protein (Howell, personal communication). This result is not currently explainable, but would suggest that the results, found in this study, are subject to the same forces as those found with DHF.

The next step for this part of the project would be to test whether R67 DHFR has the ability to utilize any of the above cofactors in a reduction reaction. To do this it must first be determined whether the presence of these cofactors would inhibit the native reduction reaction of NADPH and DHF. Inhibition would show that the variant cofactor was actually

binding in the pore of the protein. Secondly, the flavin cofactors must be changed from the oxidized form to the reduced form and also show that the cofactors are stable in solution.

CHAPTER IV

STUDIES OF THE ARTIFICIALLY ENGINEERED R67 $DHFR_{double}$

INTRODUCTION:

As previously discussed in the introduction, native R67 DHFR is active as a homo-tetramer with an unusual pore structure which is 24 Å long by 18 Å wide and passes through the center of the protein. From kinetic, ligand binding and difference Fourier mapping experiments, it has been suggested that the pore is the site of both cofactor and substrate binding. This would also suggest that native R67 DHFR has only one active site, which has been shown to possess a unique 222 symmetry, per tetramer, and that residues from each of the monomers contributes to one active site.

To investigate the substrate and cofactor binding sites more closely, site directed mutagenesis of the gene coding for native R67 DHFR will need to be done; However a single mutation in the gene would cause four mutations per homo-tetramer. In an effort to break the inevitable symmetry of native R67 DHFR and allow for single amino acid changes to be made, a gene which codes for tetrameric R67 DHFR needs to be constructed.

The first step towards the construction of a single gene

encoded tetrameric native R67 DHFR has been completed, the construction of dimeric R67 DHFR, termed R67 $DHFR_{double}$. R67 $DHFR_{double}$ has been shown to possess the essential tertiary structure of native tetrameric native R67 DHFR. This chapter will investigate the kinetic parameters of R67 $DHFR_{double}$ and also whether the R67 $DHFR_{double}$ still shows a primary isotope effect. These experiments will be compared with the experiments which have been done on native R67 DHFR to ensure that the newly constructed R67 $DHFR_{double}$ is fully active, and aid in determining if the strategy for construction was valid.

METHODS AND MATERIALS:

CONSTRUCTION AND PURIFICATION OF THE R67 $DHFR_{double}$:

The construction of the R67 $DHFR_{double}$ was performed by Ming Yin on the plasmid carrying the gene coding for a synthetic R67 DHFR, pLZ1 (described in Reece *et al.* 1991). Standard recombinant DNA procedures were performed which were followed by double stranded DNA sequencing, and Western blot analysis to ensure the recombinant DNA was correctly synthesized (Zhuang *et al.*, in press).

The R67 $DHFR_{double}$ was expressed in *E. coli* and purified by the method previously described in this thesis and by Reece *et al.* 1991, for native R67 DHFR.

KINETIC MEASUREMENTS:

Kinetic assays were run using the same manner as those

previously described for native R67 DHFR in chapter II. Subsaturating concentrations for both substrate (DHF) and cofactor (NADPH) were used in the determination of the kinetic parameters. The addition of the R67 $DHFR_{double}$ was used to initiate the assay, the initial rates of reaction were measured spectrophotometrically and the data generated from this set of experiments were fit in Enzfitter.

FLUORESCENCE QUENCHING USING NADPH:

Tryptophan fluorescence quenching with NADPH on the R67 $DHFR_{double}$ was performed in the same manner as previously described in chapter III. The intrinsic protein fluorescence of the R67 $DHFR_{double}$ was monitored with an excitation of 290 nm and an emission of 340 nm.

NADPD ISOTOPE EFFECT:

The preparation of the NADPD was carried out by the method of Viola *et al.*, 1984, and has been previously described in this thesis in chapter II. Standard subsaturating Michaelis-Menten kinetics were performed using both NADPH and NADPD on both native R67 DHFR and the R67 $DHFR_{double}$. The addition of enzyme was used to initiate the assays, the rates of reaction were measured by following the decrease in absorbance at 340, and the data generated were fit in Enzfitter.

RESULTS AND DISCUSSION:

From the subsaturating kinetic data generated (figures 12 and 25) we have shown R67 $DHFR_{double}$ to be fully active when compared (table 10) with native R67 DHFR with k_{cat}s of 1.2 and 1.3, and K_ms for DHF of 6.3 and 5.8, respectively. These results would suggest that R67 $DHFR_{double}$ shows no perturbation in the binding of substrate DHF. The K_ms for NADPH for R67 $DHFR_{double}$ have also been shown to be comparable with those determined for the native enzyme, which also suggests that R67 $DHFR_{double}$ shows no perturbation in binding the cofactor.

From the investigation of the fluorescence quenching (figure 26) done on R67 $DHFR_{double}$ we have shown the R67 $DHFR_{double}$ and native R67 DHFR to have similar K_ds and binding stoichiometries (table 11). This result would suggest that the NADPH binding site in the R67 $DHFR_{double}$ has not been perturbed in the construction of the protein and that R67 $DHFR_{double}$ has maintained the same binding interactions as the parent native R67 DHFR. Further since $K_{m(NADPH)}$ equals the $K_{d(NADPH)}$, the Michaelis constant yields a good approximation of the binding constant.

The effect of the substitution of NADPD for NADPH in the R67 $DHFR_{double}$ has also been investigated (figure 27). From Table 12, we can see that R67 $DHFR_{double}$ like R67 DHFR, shows a ^{D}V value of approximately 3. This result would suggest that R67 $DHFR_{double}$ has maintained the same rate determining step in the reduction of DHF.

From these results and the results on the structure of the R67 $DHFR_{double}$ (Zhuang *et al.*, in press), we suggest that the rationale for the plasmid construction of the R67 $DHFR_{double}$ was valid. We have also shown that the R67 $DHFR_{double}$ protein is not significantly different from native R67 DHFR in terms of the binding and dissociation of substrate and cofactor, and that the R67 $DHFR_{double}$ is fully active with k_{cat} and K_m values which match those found in native R67 DHFR.

CHAPTER V

KINETIC STUDY OF THE ABILITY OF H62C R67 DHFR TO UTILIZE ACETYL-PYRIDINE NADP$^+$ IN A TRANSHYDROGENASE REACTION

INTRODUCTION:

R67 DHFR is active as a tetramer. As discussed previously, the kinetic pH profile of R67 DHFR shows an ionization at approximately 6. From studies done on the equilibrium of R67 DHFR tetramer and dimer (Nichols *et al.*, 1992), it is believed that the observed pKa of 6 is associated with the four histidine residues (histidines have a pKa which is near neutrality) which occur at the dimer-dimer interface (see figure?). It has also been suggested these histidines along with tryptophans found at the dimer-dimer interface, appear to play an important role in the stabilization of tetrameric R67 DHFR. Ionization of these histidines could potentially destabilize the tetramer, lead to the formation of dimer, and loss of the active site pore structure.

To determine the effect the histidines have on the structure and activity of R67 DHFR, site directed mutagenesis was utilized to remove the histidines. The histidines were replaced with cysteines, which have the ability to form disulfide bonds and aid in preserving the tetrameric form of

R67 DHFR at pHs at which the histidines would be protonated. The resulting site directed mutant, known as H62C R67 DHFR (Nichols, M.S. thesis) has been shown to be stable as a tetramer at lower pHs and maintains approximately the same activity as native R67 DHFR (Holland, *et al.*, 1993) The H62C R67 DHFR, however, has been shown by fluorescence enhancement to be able to bind greater than two molecules of NADPH (Howell, unpublished observations) whereas the native R67 DHFR only possesses the ability to bind one NADPH per tetramer.

Given the unusual NADPH binding data on H62C R67 DHFR, this chapter investigates whether H62C R67 DHFR possesses the ability to catalyze a transhydrogenase reaction.

A transhydrogenase reaction involves the transfer of electrons from one cofactor to a second cofactor. Native R67 DHFR has previously been shown to be unable to carry out this type of reaction, even though the enzyme possesses the 222-symmetry in its active site pore; However H62C R67 DHFR has demonstrated the ability to bind more than one NADPH and would seem a likely candidate to possess a transhydrogenase activity.

MATERIALS AND METHODS:

PROTEIN CONSTRUCTION, ISOLATION AND PURIFICATION:

H62C R67 DHFR was generated and isolated through standard site-directed mutagenesis by E. E. Howell which can be found in R. Nichols, U.T., M.S. thesis. H62C protein purification

was carried out through cell lysis by sonication, and performing ammonium sulfate precipitation. The resulting solution is then treated over the same columns as the native R67 DHFR. The resulting H62C R67 DHFR protein is purified as a dimer. The dimer is allowed to stand at 4 °C for four to six weeks in a buffer consisting of 10 mM Tris and 1 mM EDTA, pH 8.0. This procedure allows for the formation of tetramer. The formed tetramer is then separated from the dimer by FPLC Mono Q column.

KINETIC MEASUREMENTS:

Kinetic measurements were performed in the same manner as previously described in chapter II. The substrates utilized in this chapter were acetyl-pyridine $NADP^+$ (purchased from Sigma Chemical Co.) and NADPH. The Acetyl-pyridine $NADP^+$ has an absorbance maximum at 259 nm and a molar extinction coefficient of 6,500 cm^{-1} M^{-1} (Keister, D. L. and San Pietro, A., 1959). Standard R67 kinetic measurements were performed in a MET buffer, pH 7.0 at 30 °C using varying substrate, cofactor and enzyme concentrations and following the decrease in absorbance at 340 nm for one minute. Alternatively kinetic measurements could also be followed by measuring the increasing absorbance at 259 nm.

RESULTS AND DISCUSSION:

H62C R67 DHFR has been shown to possess a transhydrogenase activity (figure 28) with a kcat of 0.4 sec^{-1} and a Km for acetyl-pyridine $NADP^+$ of 18 μM (see table 14 for complete analysis). This result suggests that H62C R67 DHFR binds the cofactor NADPH differently than native R67 DHFR or alternatively H62C R67 DHFR binds NADPH the same way but with a different stoiciometry.

From the kinetic, fluorometric (Howell and Linn, unpublished observations), and altered activity of H62C R67 DHFR, it is apparent that the construction of the disulfide linked dimer of R67 DHFR has significantly altered the binding properties of the enzyme. From the analysis currently being performed in the our laboratory, we have seen the H62C R67 DHFR exhibits a marked substrate and cofactor inhibition, the ability to bind more than one NADPH, and now possesses the ability to utilize NADPH and acetyl-pyridine $NADP^+$ in a reduction reaction. These observations are consistant with the alteration of the binding stoichometry for NADPH from one to greater than or equal to 2. The exact number of binding sites will be assessed by future equilibrium dialysis studies using ^3H-NADPH.

CHAPTER VI

SUMMARY OF STUDY

This study has shown R67 DHFR to be able to utilize a wider variety of substrates and bind a larger number of cofactors than its chromosomal counterpart wt. *E. coli* DHFR. We have shown R67 DHFR to possess the ability to utilize DHF, q-DMP, MTHF, DHB and DCPIP, while wt. *E. coli* DHFR only has the ability to utilize DHF and DHB. These results would suggest that R67 DHFR could be a less well evolved or a more primitive enzyme than wt. *E. coli* DHFR, and might also help in explaining the unique structure found in R67 DHFR. R67 DHFR does not contain a specific active site. Instead R67 DHFR possesses a large pore in the center of the molecule which is be where both the substrate and cofactor bind. The ability of R67 DHFR to both bind and utilize other substrates and cofactors may in part exist because of the size of the pore. Another possible conclusion which can be made from the substrate and cofactor tolerance studies performed is that Stone and Smith's hypothesis that R67 DHFR did not evolve from chromosomal DHFR, but from another nonspecific oxidoreductase, could be more likely given the results found in this study.

From investigating whether DHPR could utilize MTHF as a

substrate in a reduction reaction, we have uncovered a possible link between DHPR, R67 DHFR, and MTHFR. It has previously been shown that MTHFR possess the ability to reduce both MTHF and q-DMP (which is the known substrate for DHPR and from this study a substrate for R67 DHFR). This study has shown that the reverse is also true, DHPR has the ability to utilize MTHF as a substrate (table 13). These results, which show that R67 DHFR, DHPR and MTHFR all possess the ability to utilize q-DMP, and MTHF, might suggest that all three enzymes are be utilizing similar reduction methods for both substrates. This again suggests that R67 DHFR is a primitive enzyme which originated from a cell's need to reduce a variety of substrates. Most cells require three different enzymes to reduce DHF, q-DMP, and MTHF. R67 DHFR, however, has the ability to reduce all three substrates, which would suggest that R67 DHFR may be a primitive enzyme solicited by a cell for the reduction of more than one substrate.

These studies may also aid in supporting the proposed mechanism (figure 3) of the R67 DHFR catalyzed reduction of DHF. The proposed mechanism for the reduction is believed to be facilitated by the enzyme binding a protonated substrate. From previous studies folate has been shown to be unable to be utilized by R67 DHFR. The conclusion from this experiment was that folate is not a substrate for R67 DHFR because folate has an unobtainable pKa in solution of approximately -1.8 (Poe, 1977), and therefore a large population of protonated

substrate can not be obtained in solution. On the other hand, from this study we have shown that q-DMP, MTHF and DCPIP can be utilized by R67 DHFR in a reduction reaction. Interestingly, all three substrates possess a pKa which is obtainable in solution (5.15, 3.2, and 5.7 respectively). The results from these experiments (which were done at a pH of 7.0) would suggest that the solutions contained a relatively large population of protonated substrates, when compared to the protonated population of folate at pH 7.0, and therefore would suggest than R67 DHFR was able to bind and utilize each of the substrates in their protonated form.

From the experiments done on the R67 $DHFR_{double}$ we can conclude that the rationale for the design of the protein was sound. R67 $DHFR_{double}$ shows kinetic and fluorometric parameters which are nearly identical to those which have been determined for the R67 $DHFR_{native}$. These experiments have shown that the R67 $DHFR_{double}$ has not significantly altered any of the binding or kinetic properties of the enzyme from the native enzyme.

The experiments currently being conducted on the H62C R67 DHFR enzyme have shown that engineering a disulfide bond at the dimer-dimer interface of R67 DHFR has significantly altered the function of the protein. This enzyme now possesses the ability to utilize acetyl-pyridine $NADP^+$, a substrate which has been shown to unable to be utilized by R67 DHFR. H62C R67 DHFR also shows a marked substrate and cofactor inhibition which is not found to be present in the

native enzyme. Fluorometric studies done on H62C R67 DHFR have shown that this enzyme now possesses the ability to bind more than one NADPH, another difference from the native R67 DHFR. A pH profile of H62C R67 DHFR shows the enzyme to possess a pKa of approximately 6.1. From all of the current studies of H62C R67 DHFR, it can be concluded that this enzyme is significantly different from native R67 DHFR.

LIST OF REFERENCES

Amyes, S.G.B., and Smith, J.T., (1974), *Biochem. Biophys. Res. Comm.*, 58: 412-418

Amyes, S.G.B., (1989), *J. Med. Microbiol.*, 28: 73-83

Amyes, S.G.B., and Towner, K.J. (1990), *J. Med. Microbiol.*, 31: 1-20

Amyes, S.G.B., and Gemmel, C.G., (1992), *J. Med. Microbiol.*, 386: 4-29

Armarego, W.L.F., Randles, D., and Taguchi, H., (1983), *Biochem. J.*, 211: 357-361

Armarego, W.L.F., (1989) *Chemistry and Biology of Pteridines*, Curtis, H., Ghisla, S., and Blau, N., Eds., Walter de Gruyter, Berlin (1990)

Ayling, J.E., *et al.*, (1989), *Chemistry and Biology of Pteridines*, pp. 43-48

Bailey, S.W., and Ayling, J.E., (1983), *Biochemistry*, 22: 1790-1798

Blakley, R.L, (1969) *The Biochemistry of Folic Acid and Related Pteridines*, North Amsterdam, Holland

Blakley, R.L., (1984) *Folates and Pteridines: Chemistry and Biochemistry of Folates*, (Blakely, R.L., and Benkovic, S.J., Eds.), Vol. I, pp 190-250, Wiley, New York

Broad, D.F., and Smith, J.T., (1982), *Eur. J. Biochem.*, 125: 617-622

Castano, E.M., and Frangione, B., (1988), *Lab. Invest.*, 58: 122-132

Craine, J.E., Hall, E.S., and Kaufman, S., (1972), *J. Biol. Chem.*, 6082-6091

Cleland, W. W., (1963), *Boichim. Biophys. Acta*, 67: 104-137

Donaldson, K.O., and Keresztesy, J.C., (1962), *J. Biol. Chem.*, 237: 3815-1904

Fleming, M.P., Datta, N., and Gruneberg, R.N., (1972), *Br. Med. J.*, 1:726-728

Flensburg, J., and Steen, R., (1986), *Nucleic Acids Res.*, 14: 5933-5935

Gurr, E., (1960), Congo red. In *Encyclopedia of Microscopic Stains*, pp. 140-141, Leonard Hill, London

Hitchings, G.H., Ed, (1983) *Inhibition of Folate Metabolism in Chemotherapy*, pp 1-23, Springer-Verlag, New York

Hitchings, G.H., and Baccanari, D.P., (1984) *Folate Antagonists as Theraputic Agents*, (Sirontnak, F.M., Burchall, J.J., Ensminger, W.B., and Montgomery, J.A., Eds.) Vol. I, pp 150-174, Academic Press, Orlando

Holland, J.C., *et al.*, (in press) *The Chemistry and Biology of Pteridines 1993*, Mobile, Alabama

Howell, E.E., Villafranca, J.E., Warren, M.S., Oatley, S. J., and Kraut, J., (1986), *Science*, 231: 1123-1128

Jannsson, C., and Skold, O., (1991) *Antimicrob. Agents in Chemother.*, 35: 1891-1899

Joyner, S.S., Fling, M.E., Stone, D., and Baccanari,D.P., (1984) *J. Biol. Chem.*, 259: 5851-5856

Kallen, R.G., Viale, R.O., and Simth, L.K., (1972), *Journal of the American Chemical Society*, 94: 2: 576-581

Kaufman, S. and Fisher, D.B., (1974), in Molecular Mechanisms of Oxygen Activation, Hayaishi, O., Ed., pp. 285-368

Keister, D. L. and San Pietro, A., (1959), *Biochem. Biophys. Res. Comm.*, 1:110-113

Kraut, J., and Matthews, D.A., (1987), *Biological Macromolecules and Assembles*, Jurnak, F.A., and McPherson, A., Eds., Vol. III, pp 1-71, Wiley, New York

Kutzbach, C., and Stakstad, E.L.R., (1971), *Biochim. Biophys. Acta*, 250: 459-477

Matthews, D.A., Smith, S.L., Baccanari, D.P., Burchall, J.J., Oately, S.J., and Kraut, J. (1986) *Biochemistry*, 25: 4194-4204

Matthews, D.A., *et. al.*, (1991), *Archives of Biochemistry and Biophysics*, 287: 234-239

Matthews, R.G., and Haywood, B.J., (1979), *Biochemistry*, 19: 4845-4851

Matthews, R.G., and Kaufman, S., (1980), *J. Biol. Chem.*, 255: 6014-6017

Morrison J.F. and Sneddon, M.K. (1990) in Chemistry and Biology of Pteridines 1989, Curtius, H.-Ch., Ghisla, S., and Blau, N., Eds., pp 727-733, Water de Gruyter, Berlin

Nichols, *et al.*, (1993), *Biochemistry*, 32: 1695-1706

Nielson, *et al.*, (1969), *Eur. J. Biochem.*, 9: 497-505

Pattishall, K.H., Acar, J., Burchall, J.J., Goldstein, F.W., and Harvey, R.J., (1977), *J. Biol. Chem.*, 252:2319-2325

Poe, M., (1977), *J. Biol. Chem.*, 252: 3724

Reece, L.J., Nichols, R., Ogden, R.C., and Howell, E.E., (1991), *Biochemistry*, 30: 10904-10895

Smith, G.K., and Nichol, C.A., (1986), *J. Biol. Chem.*, 54: 729-764

Stone, D., and Smith, S.L, (1979), *J. Biol. Chem.*, 254: 10857-10861

Stone, D., and Morrison, J.F., (1988), *Biochemistry*, 27: 5493-5499

Sueoka, T., Hikita, H., and Katoh, S., (1990), *Enyzmology and Molecular Biology of Carbonyl Metabolism 3*, pp.229-239

Sundstrom, L., Vanyagamoorthy, T., and Slold, O., (1987), *Antimicrob. Agents in Chemother.*, 31: 60-66

Swift, G., McCarthy, B.J., and Heffron, F., (1981), *Mol. Gen. Genet.*, 181: 441-447

Tamura, J.K., Rakov, R.D., and Cross R.L., (1986), *J. Biol. Chem.*, 261: 4126-4133

Thompson, C.J., Young H.K., and Amyes, S.G.B., (1990), *J. Med. Microbiol.*, 32: 153-158

Turnell, W.G., and Flinch, J.T., (1992), *J. Mol. Bio.*, 227:1205-1223

Varughese, K.I., (1992), *Biochemistry*, 32: pp: 1129-1137

Vermerch, P.S., and Bennett, G.N., (1986), *Gene*, 41: 289 -297

Weber, S., and Whiteley, J.M., (1985), *Archives of Biochemistry and Biophysics*, 236: 681-690

Wylie, B.A., and Koornhof, H.J., (1991), *J. Med. Microbiol.*, 35: 214-218

Young, H.K., and Amyes, S.G.B., (1986) *J. Biol. Chem.*, 261: 2503-2505

Zhuang, P., *et al.*, (1993), *J. Biol. Chem.*, in press

Zolg, J.W., and Hanggi, U.J., (1981), *Nucleic Acids Res.*, 9: 697-710

APPENDIX

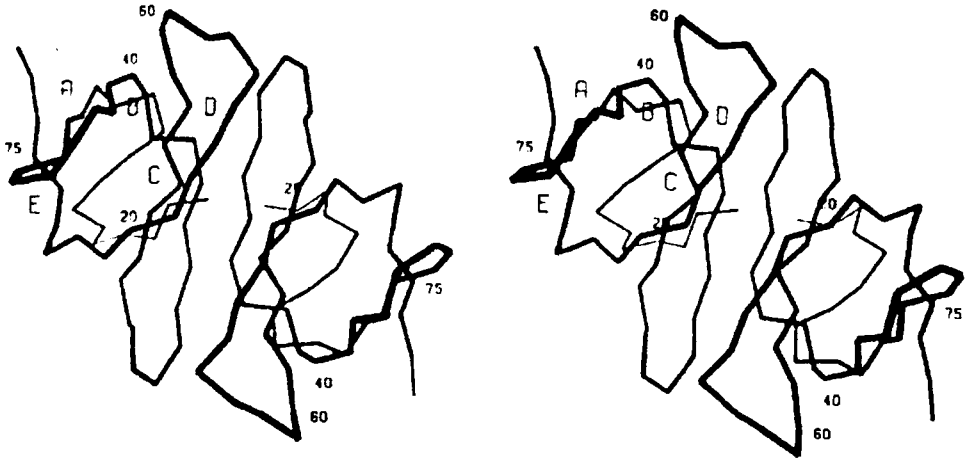

Figure 1: Crystal structure of R67 DHFR dimeric form. Diagram shows the α carbon backbone of the R67 DHFR dimer. Reprinted from Matthews et al. 1986

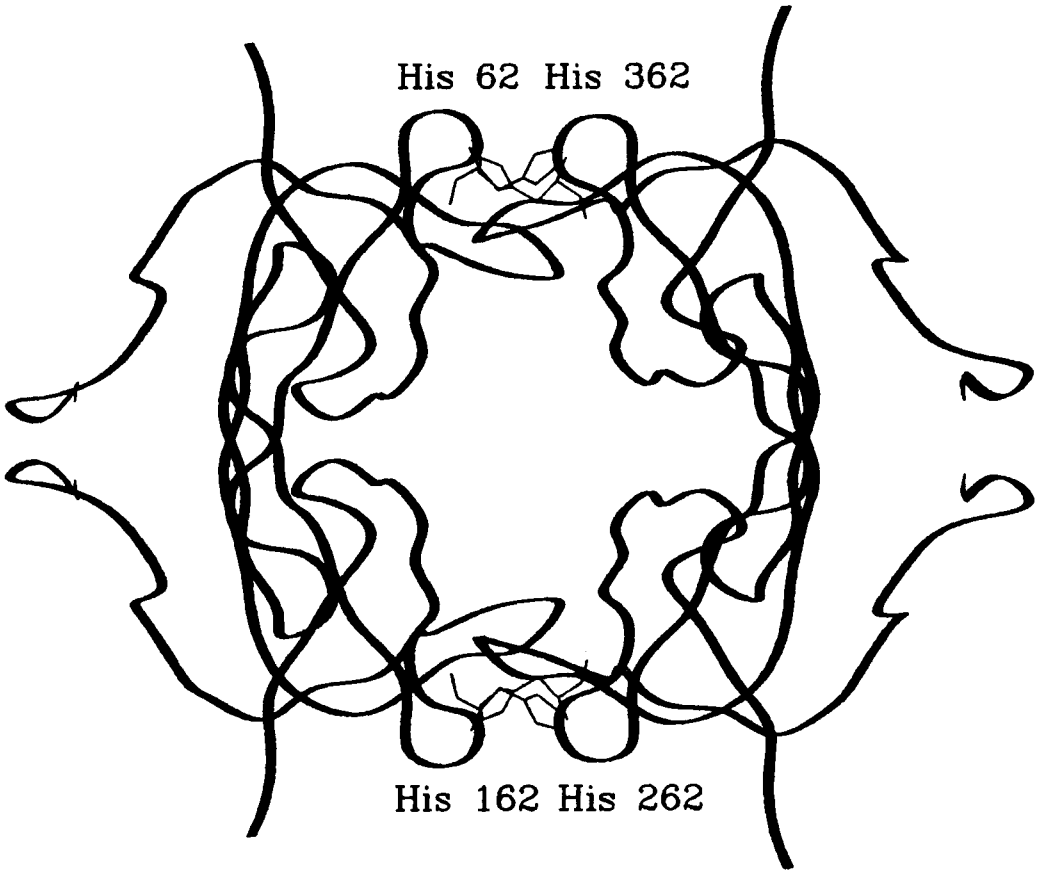

Figure 2: Tetrameric R67 DHFR. Location of histidine residues found at the dimer-dimer interfaces.

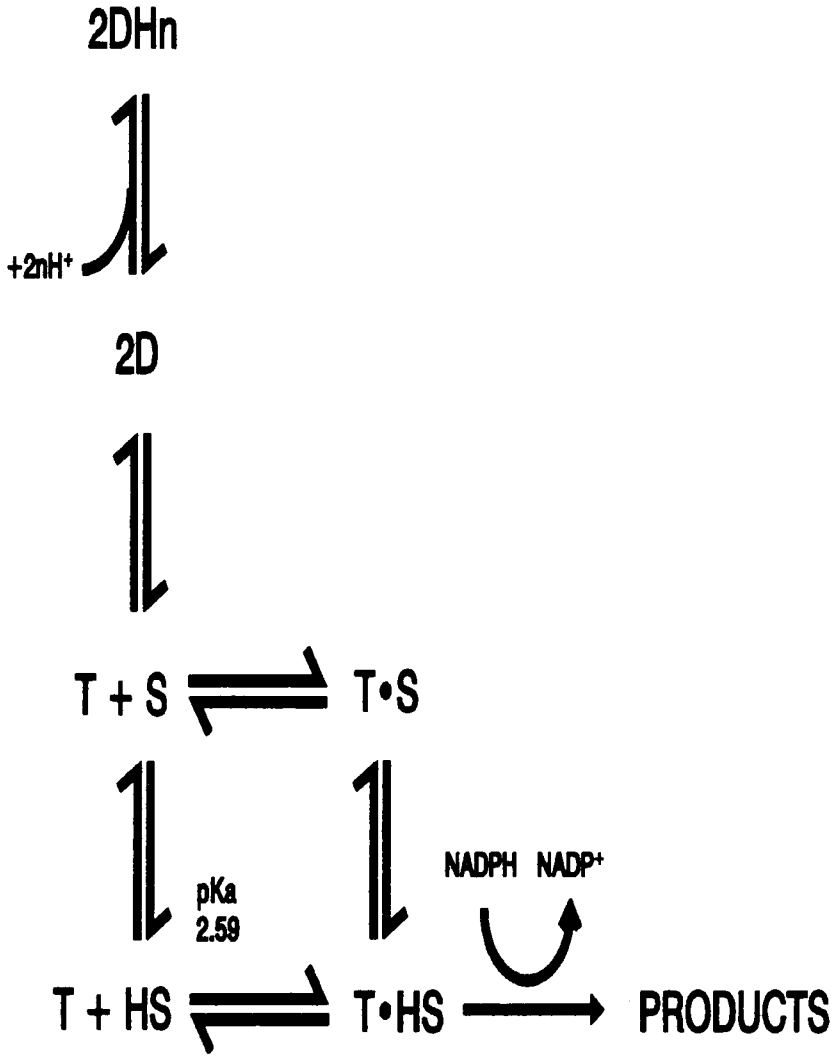

Figure 3: Proposed reaction mechanism of R67 DHFR for the reduction of DHF. T represents the R67 DHFR tetramer, D represents the R67 DHFR dimer, S represents the substrate, and HS represents the protonated substrate.

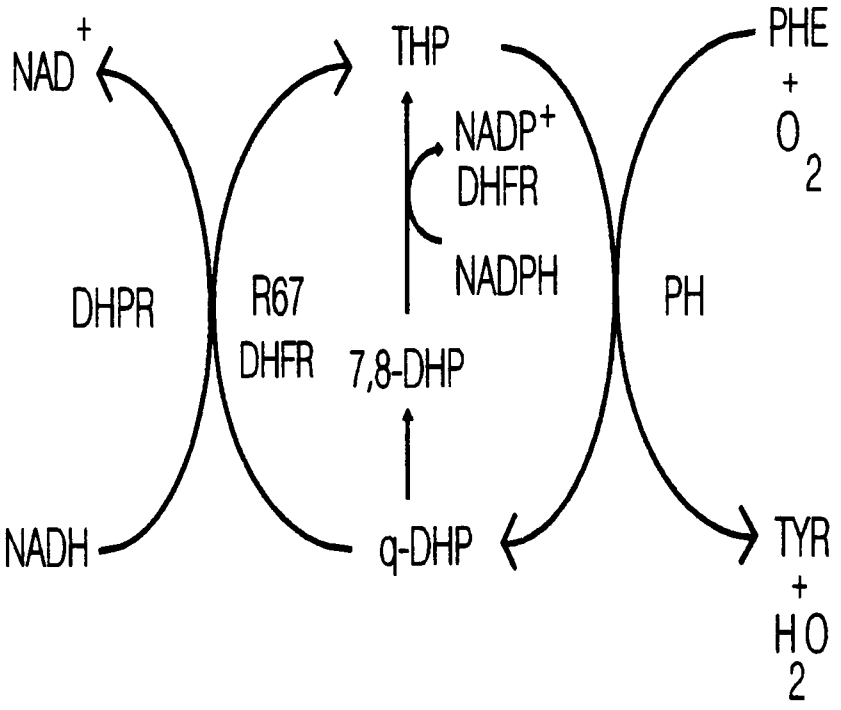

Figure 4: Oxidation/reduction of THP, and generation/ degradation of q-DMP at pH of 7.0. PH represents phenylalanine hydroxylase, Tyr represents tyrosine, and Phe represents phenylalanine.

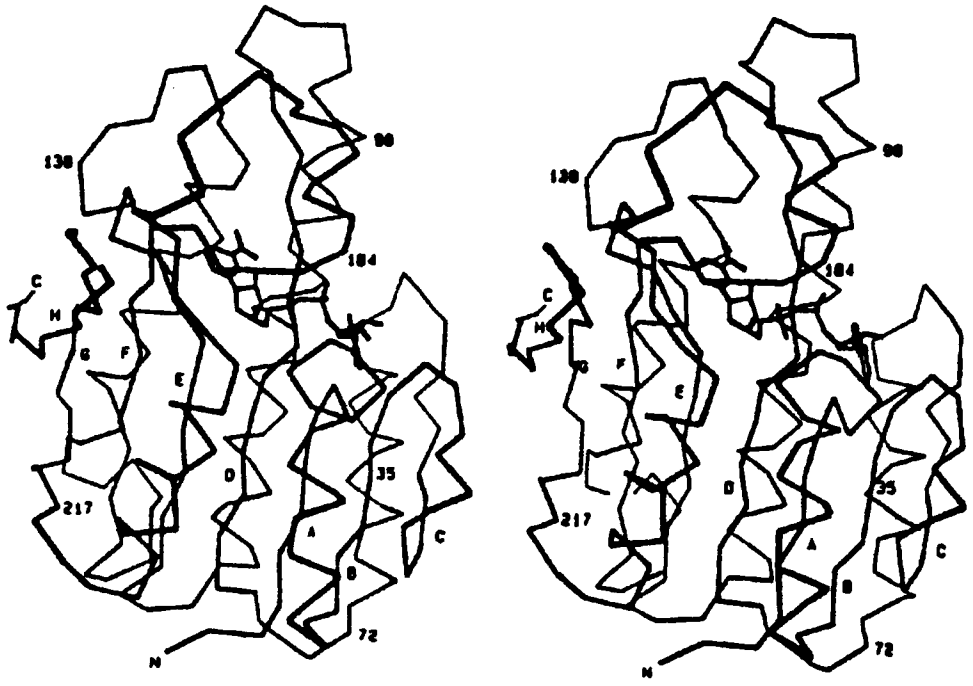

Figure 5: Crystal structure of DHPR. Source: Matthews *et al.*, 1992

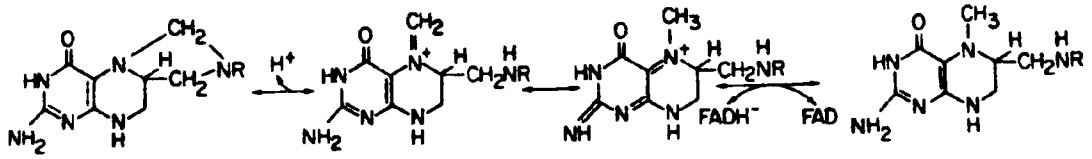

Figure 6: Proposed mechanism for the MTHFR catalyzed reduction of MTHF. Reprinted from Matthews, *et al.*, 1986

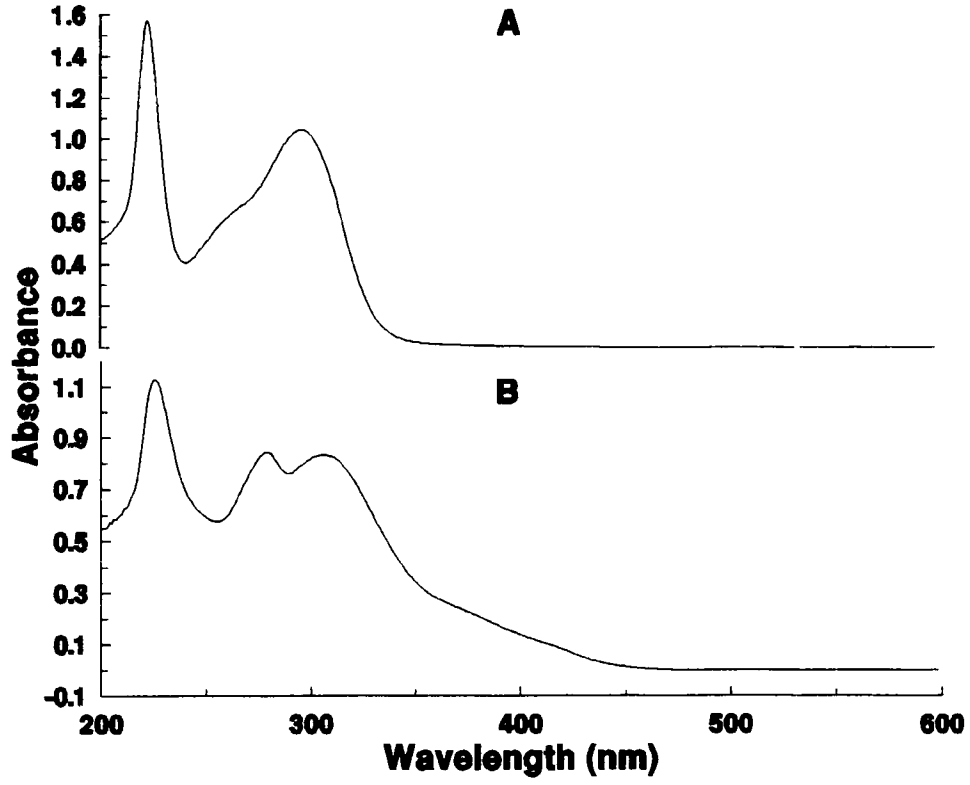

Figure 7: Absorbance scans from the generation of q-DMP. A. Shows the absorbance scan of THP before the addition and incubation with peroxide and peroxidase. B. Shows the absorbance scan of THP afterthe additions of peroxide and peroxidase.

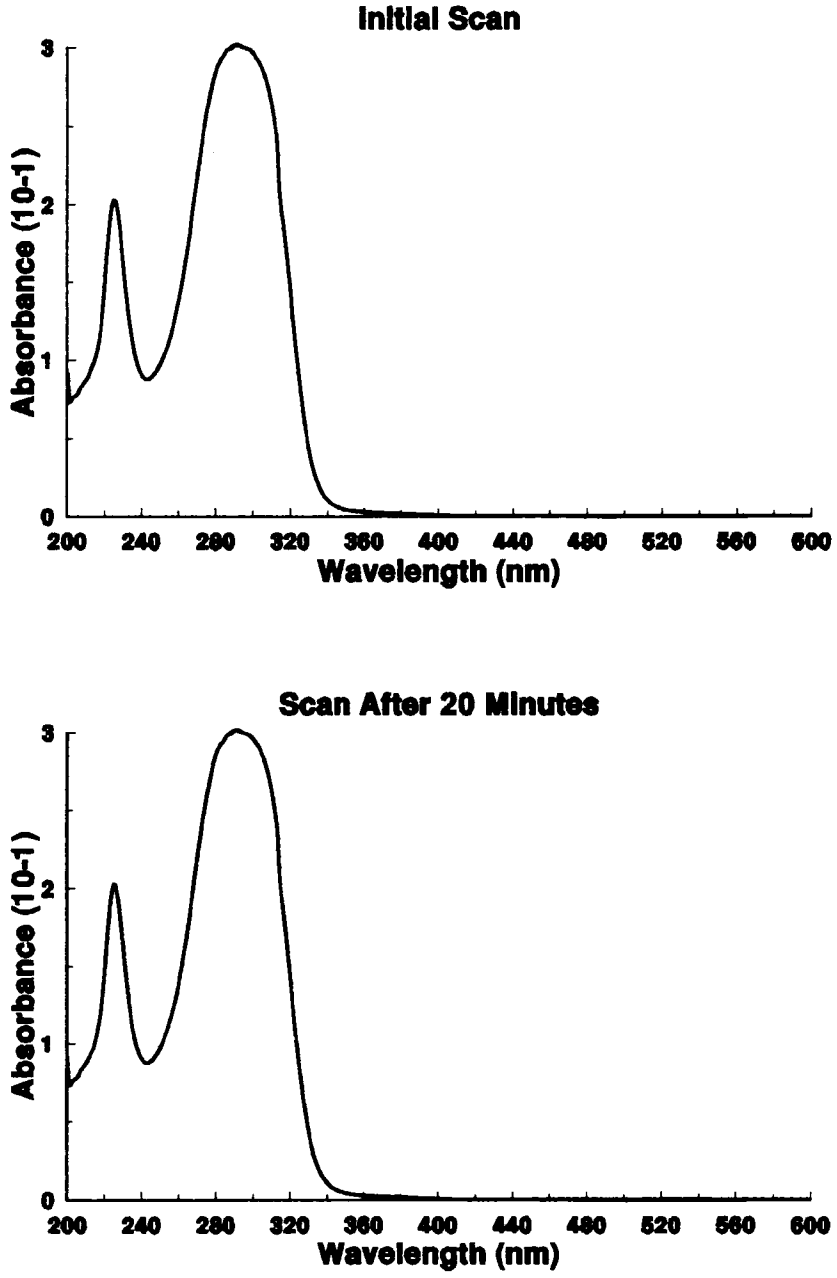

Figure 8: Absorbance scans of MTHF. Top scan shows the inital absorbance scan for MTHF. Bottom scan shows absorbance profile of MTHF 20 minutes after resuspension.

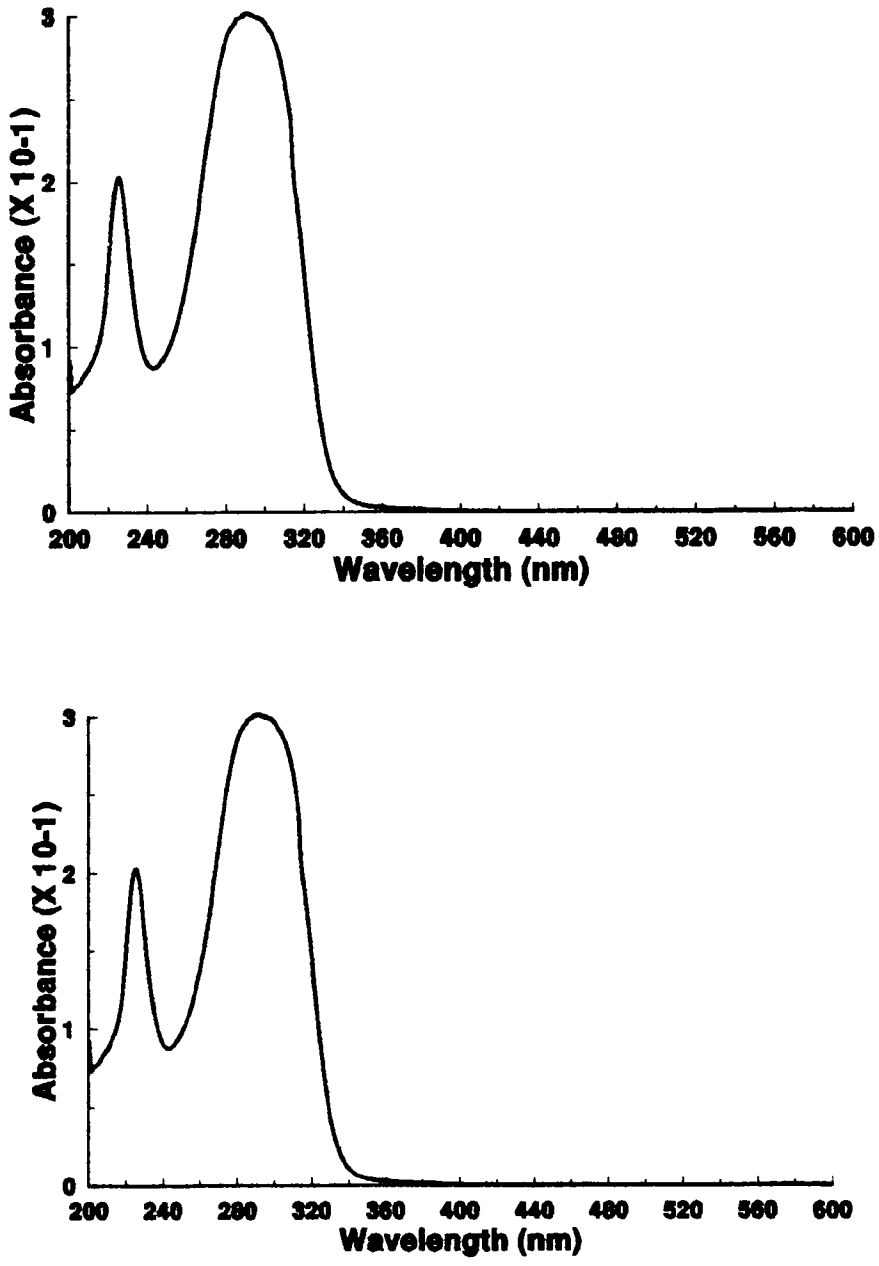

Figure 9: Absorbance scans of MeTHF. Top scan shows the inital absorbance scan for MeTHF. Bottom scan shows absorbance profile of MeTHF 30 minutes after anaerobic resuspension in MET buffer pH 7.0

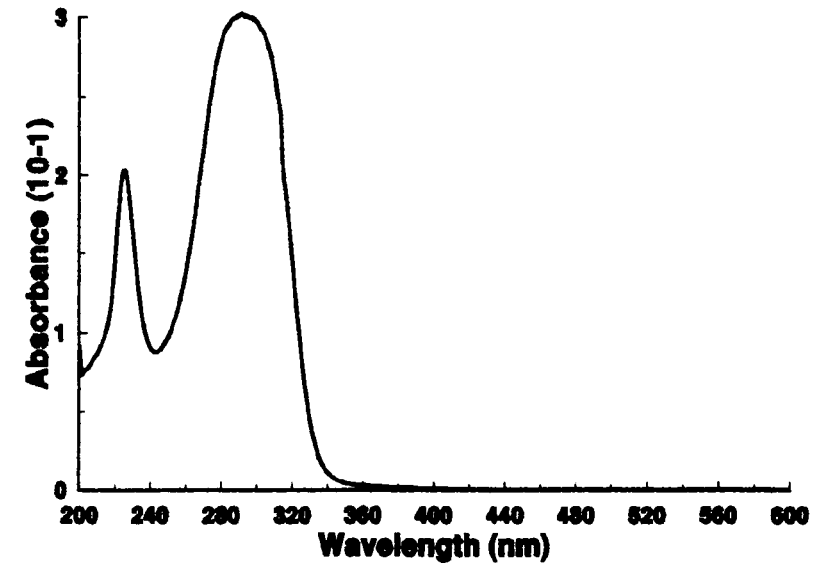

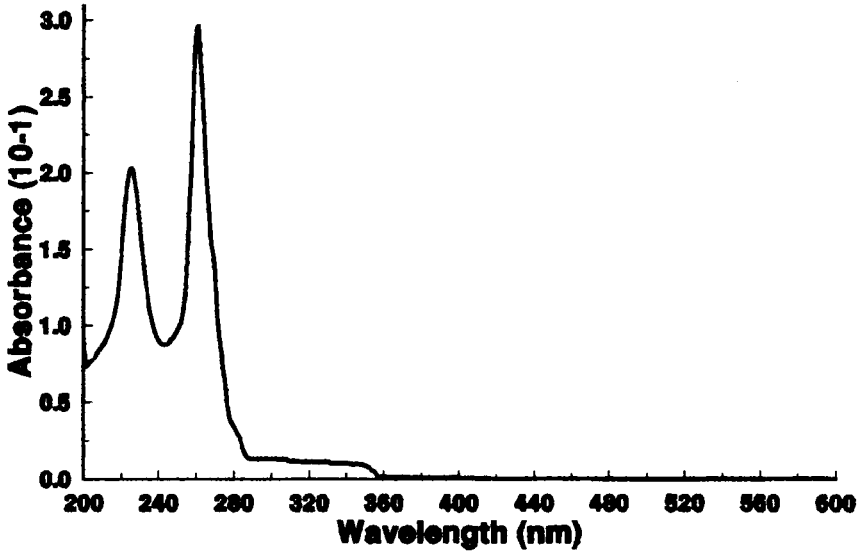

Figure 10: Absorbance scans for the formation of FTHF. Top scan shows the initial absorbance profile of starting compound, MeTHF. Bottom scan shows the absorbance profile from the formation of FTHF.

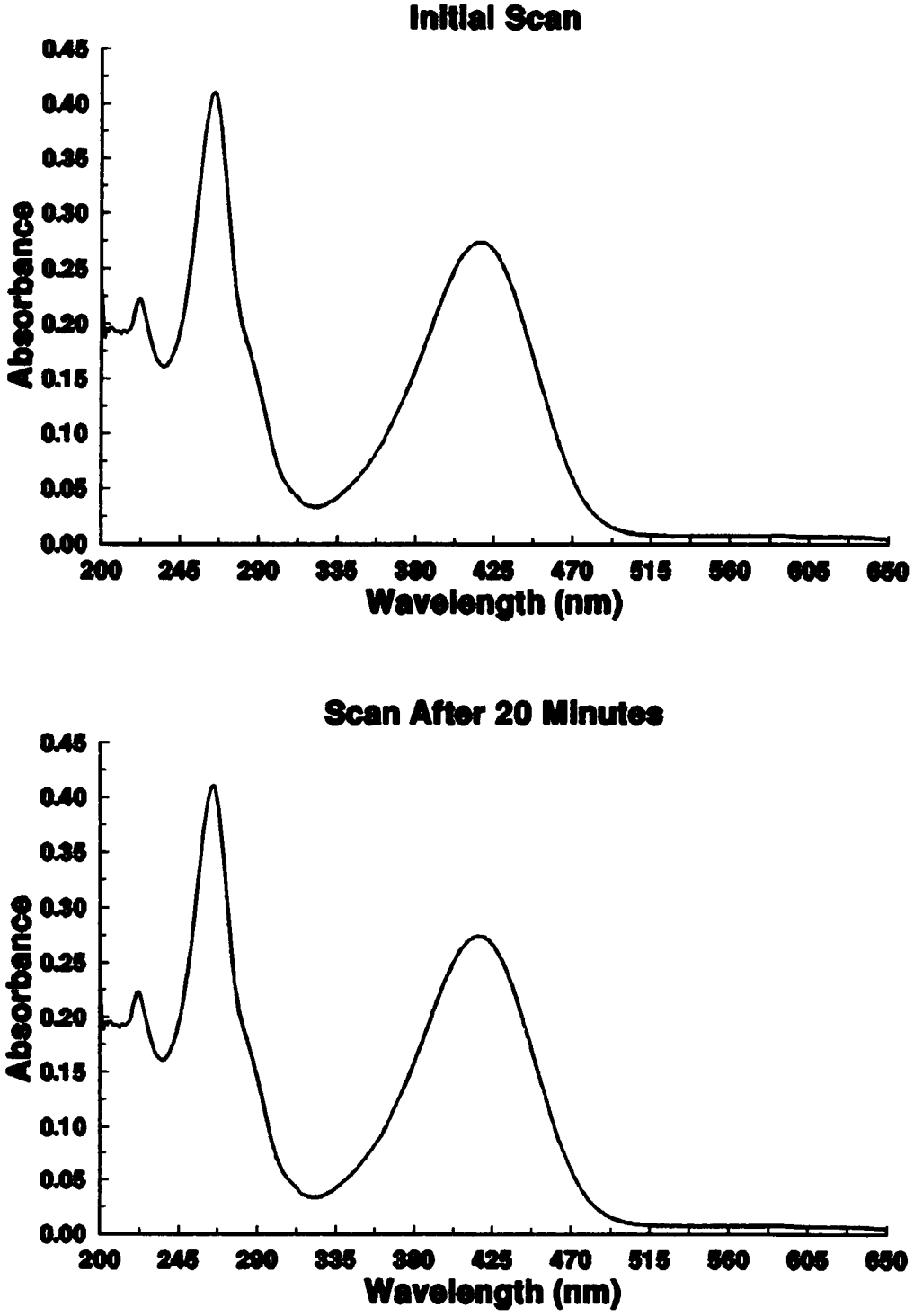

Figure 11: Absorbance scans for sepiapterin. Top scan shows the initial absorbance profile of sepiapterin. Bottom scan shows the absorbance profile of sepiapterin 20 minutes after being resuspended in MET buffer pH 7.0.

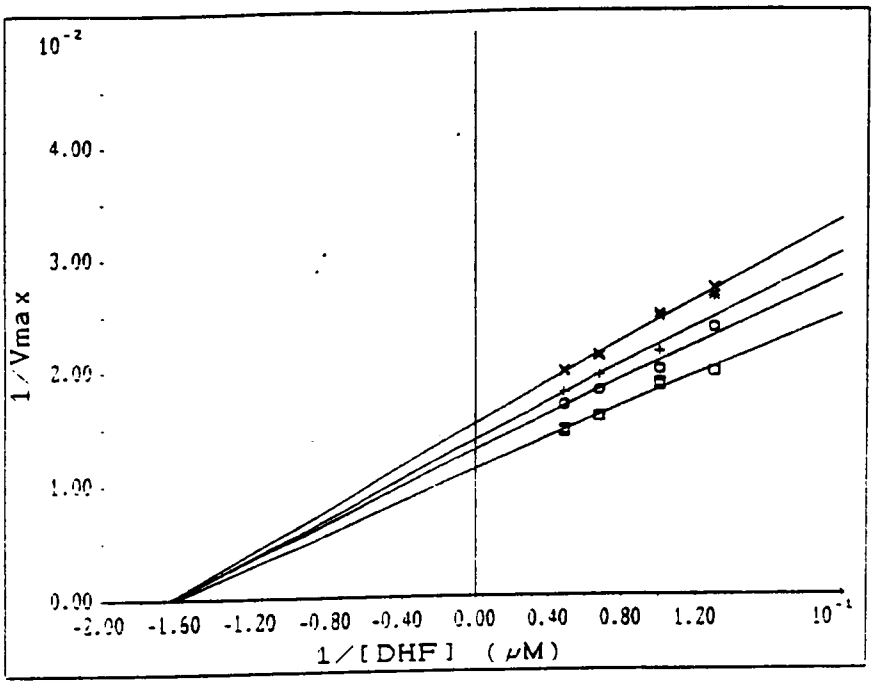

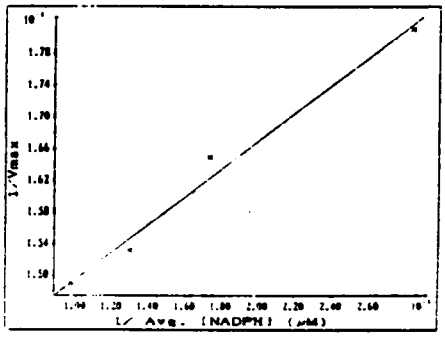

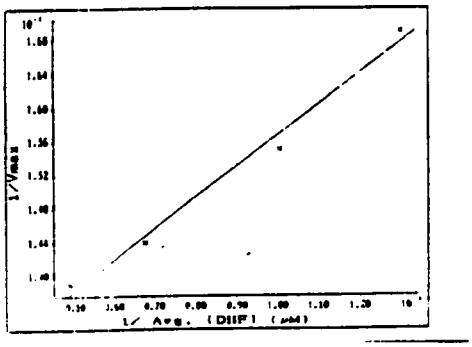

Figure 12: Michaelis-Menten kinetics from the R67 DHFR catalyzed reduction of DHF. Figure shows typical Lineweaver-Burke plot of 1/v vs. 1/substrate. From the secondary replots both k_{cat} and K_m have been determined.

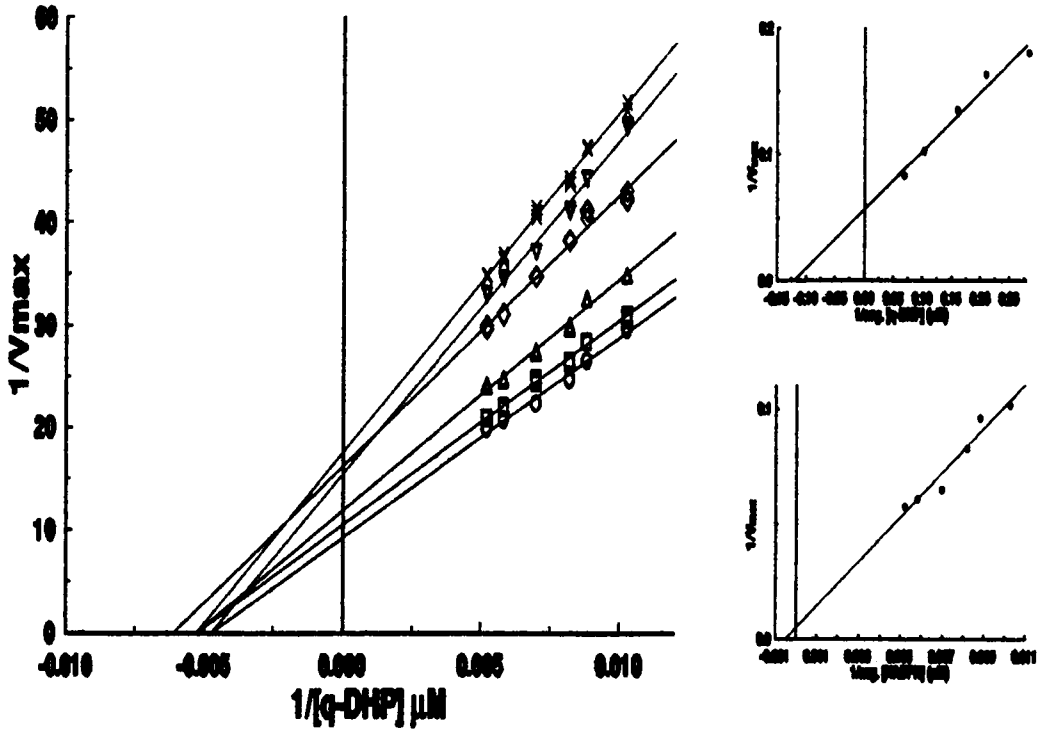

Figure 13: Michaelis-Menten subsaturating kinetics from the R67 DHFR catalyzed reduction of q-DMP.

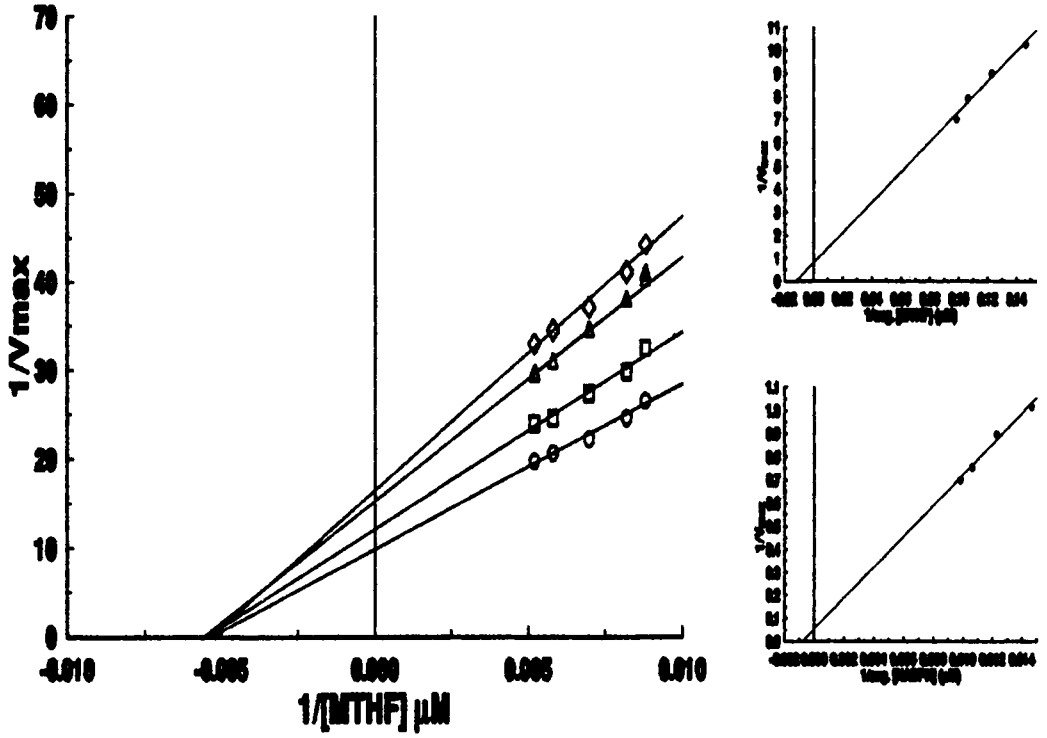

Figure 14: Michaelis-Menten subsaturating kinetics from the R67 DHFR catalyzed reduction of MTHF.

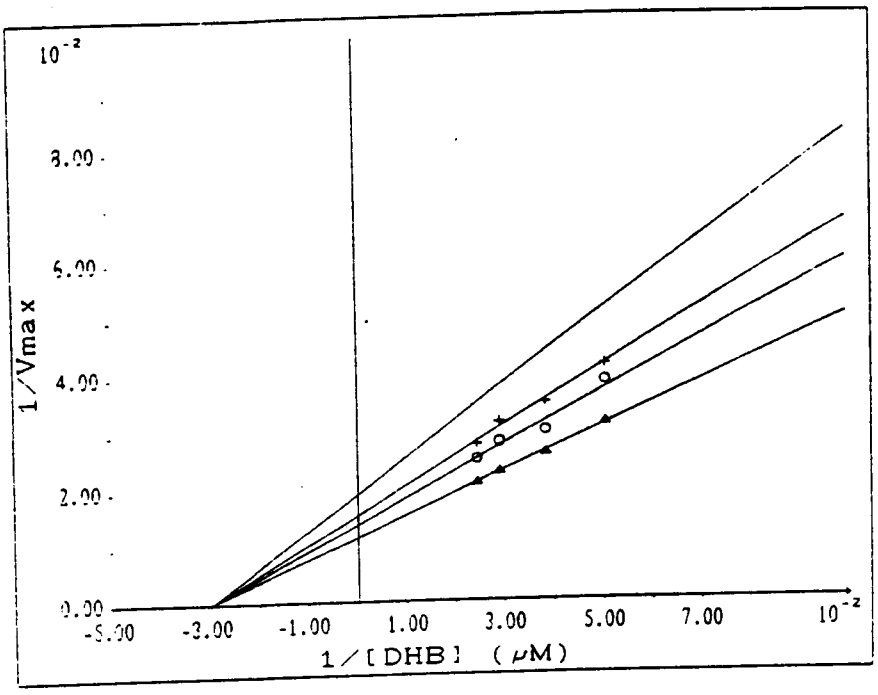

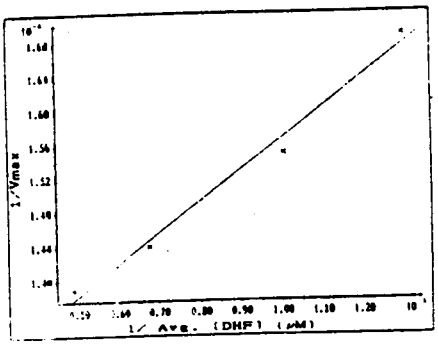

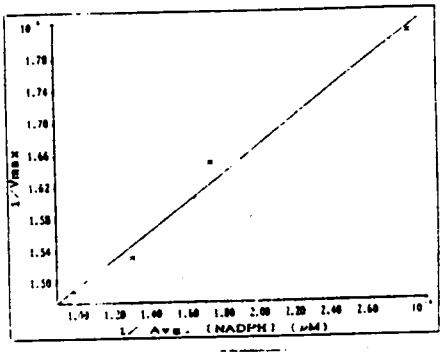

Figure 15: Michaelis-Menten subsaturating kinetics from the R67 DHFR catalyzed reduction of DHB.

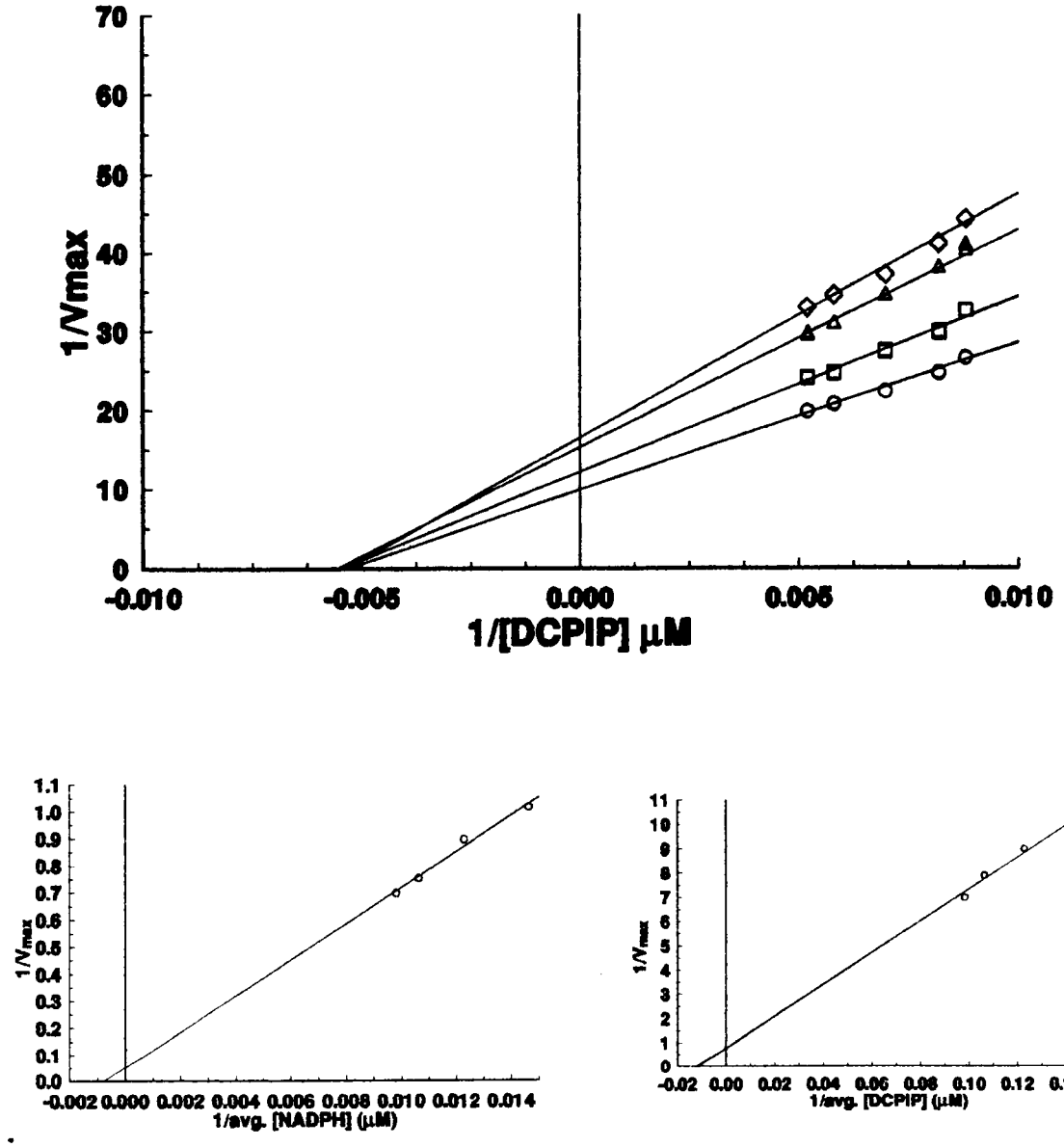

Figure 16: Michaelis-Menten subsaturating kinetics from the R67 DHFR catalyzed reduction of DCPIP.

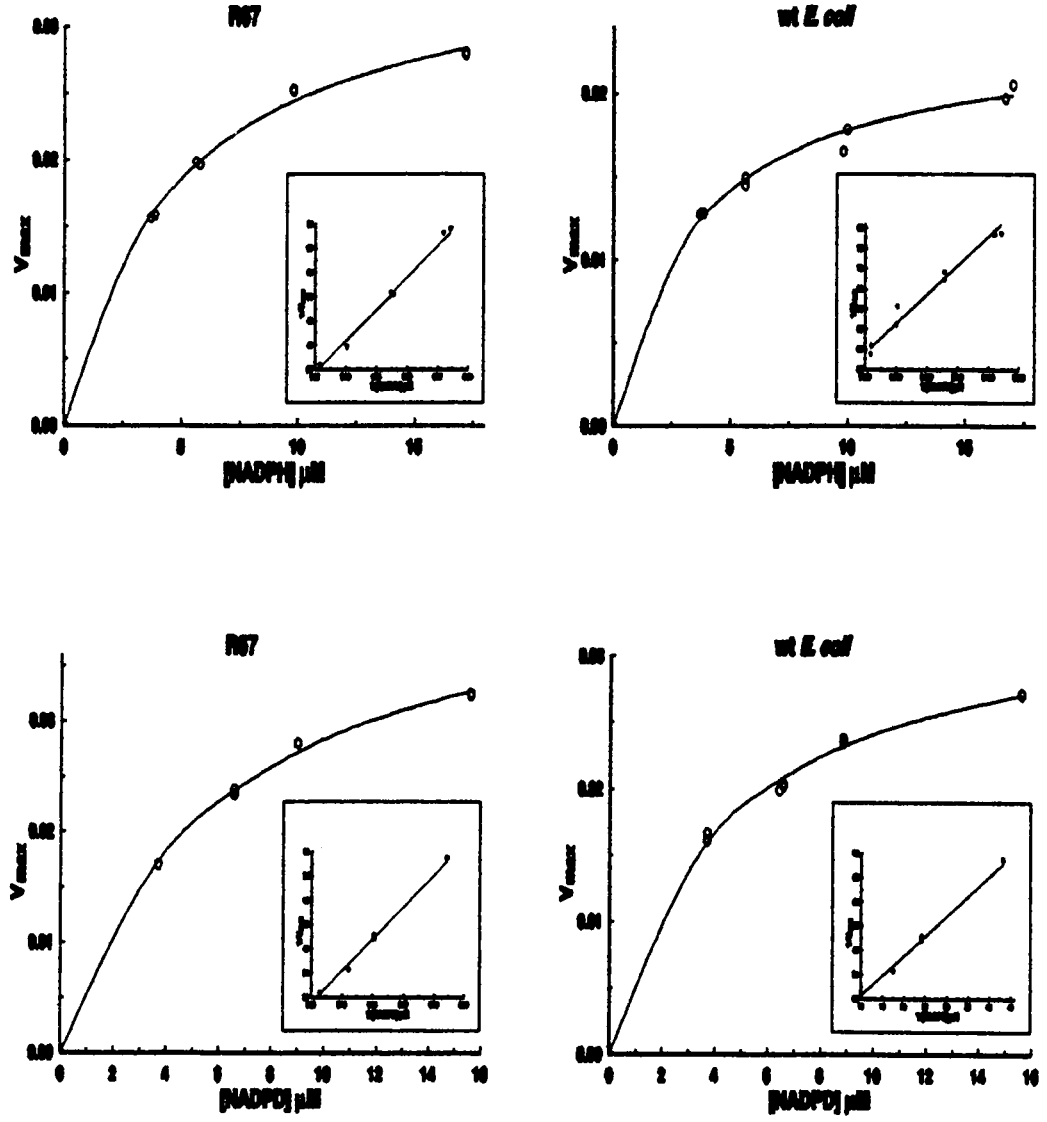

Figure 17: Michaelis-Menten kinetics from the R67 DHFR and wt. *E.coli* DHFR catalyzed reduction of DHB using NADPD or NADPH as the cofactor.

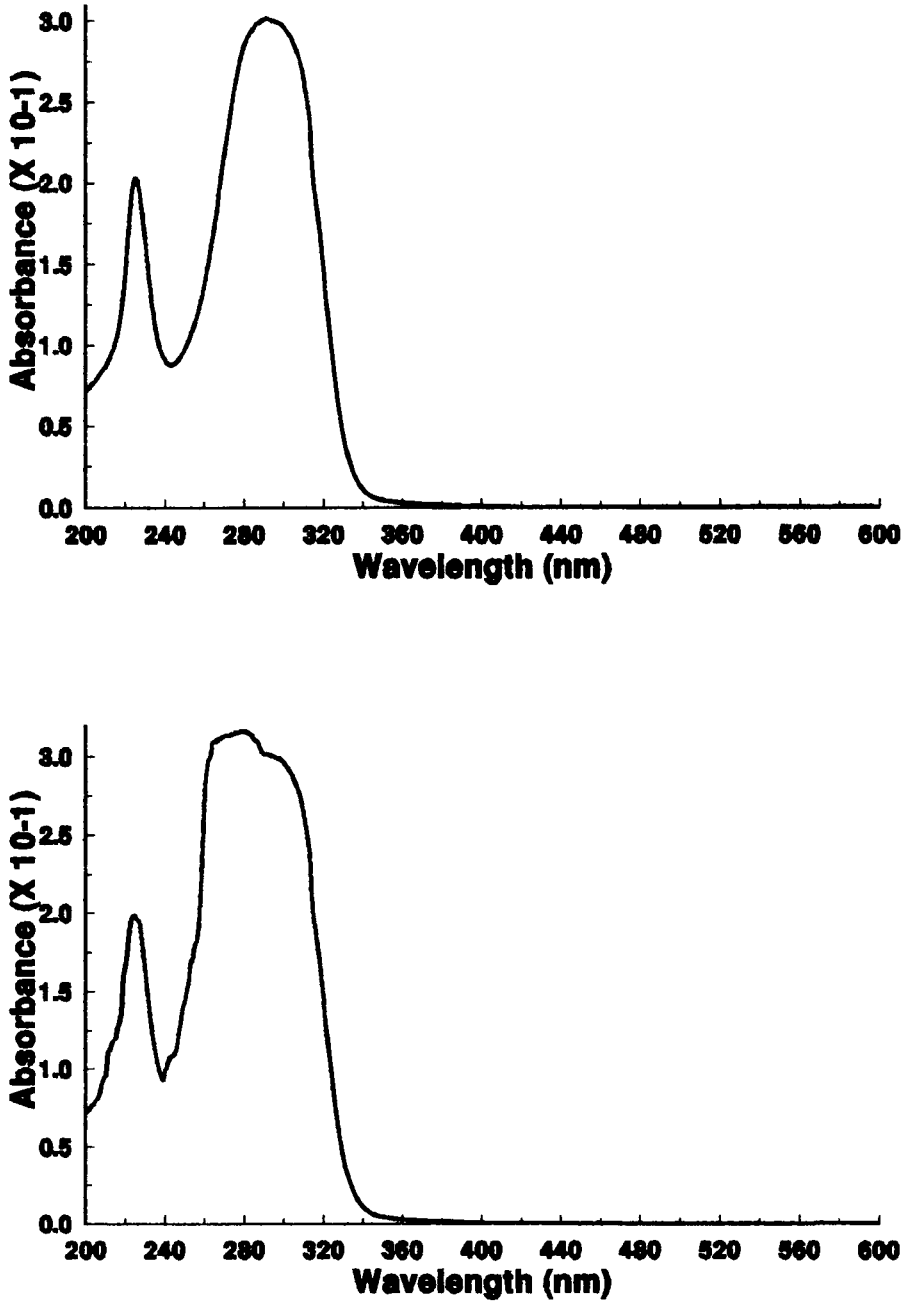

Figure 18: Absorbance scans for PLP-AMP. Top scan shows the initial absorbance profile of PLP-AMP (60 μM) before the addition of protein. Bottom scan shows the absorbance profile of PLP-AMP after the addition of protein (3 μM).

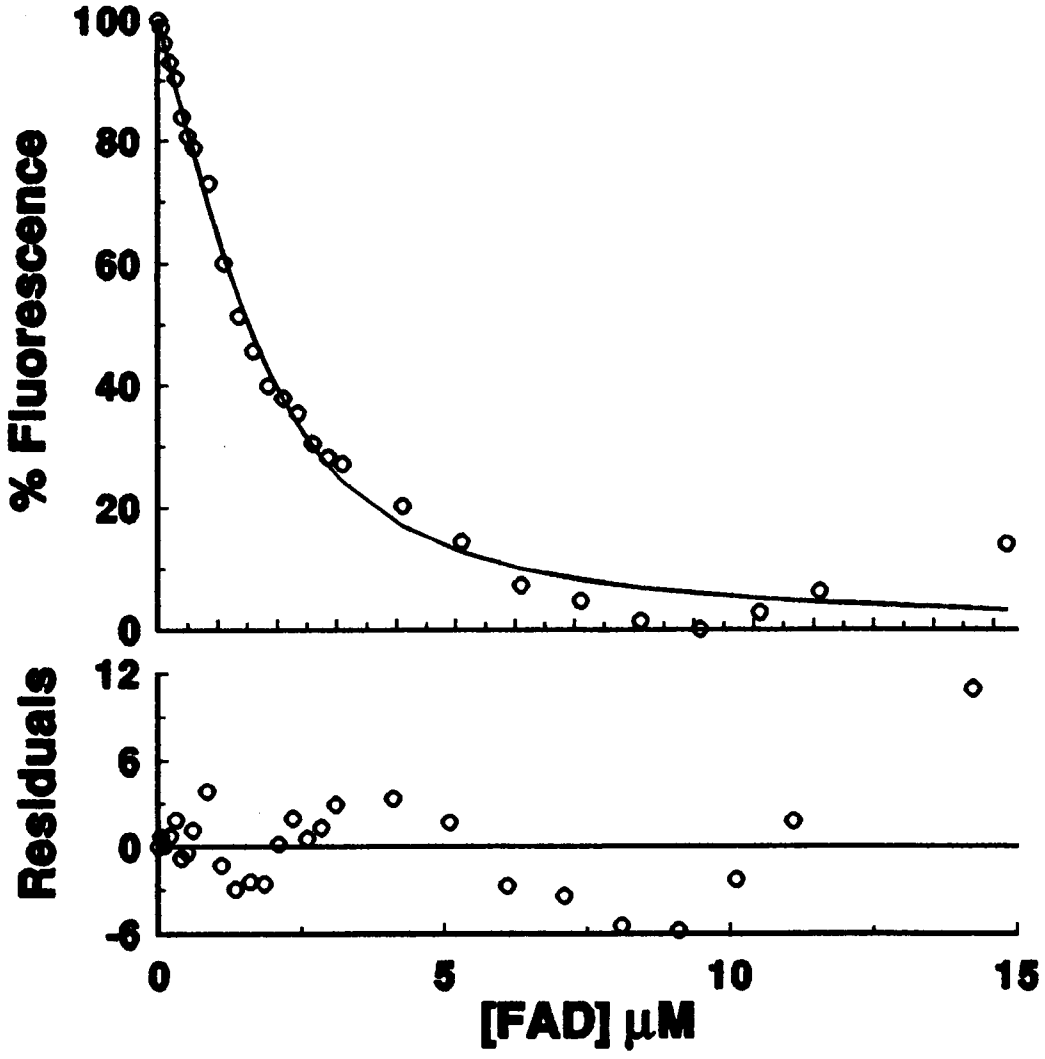

Figure 19: Fluorescence quenching of tryptophan residues in R67 DHFR using FAD as the ligand. Experiment was performed with an excitation wavelength of 290 nm and an emission wavelength of 340 nm.

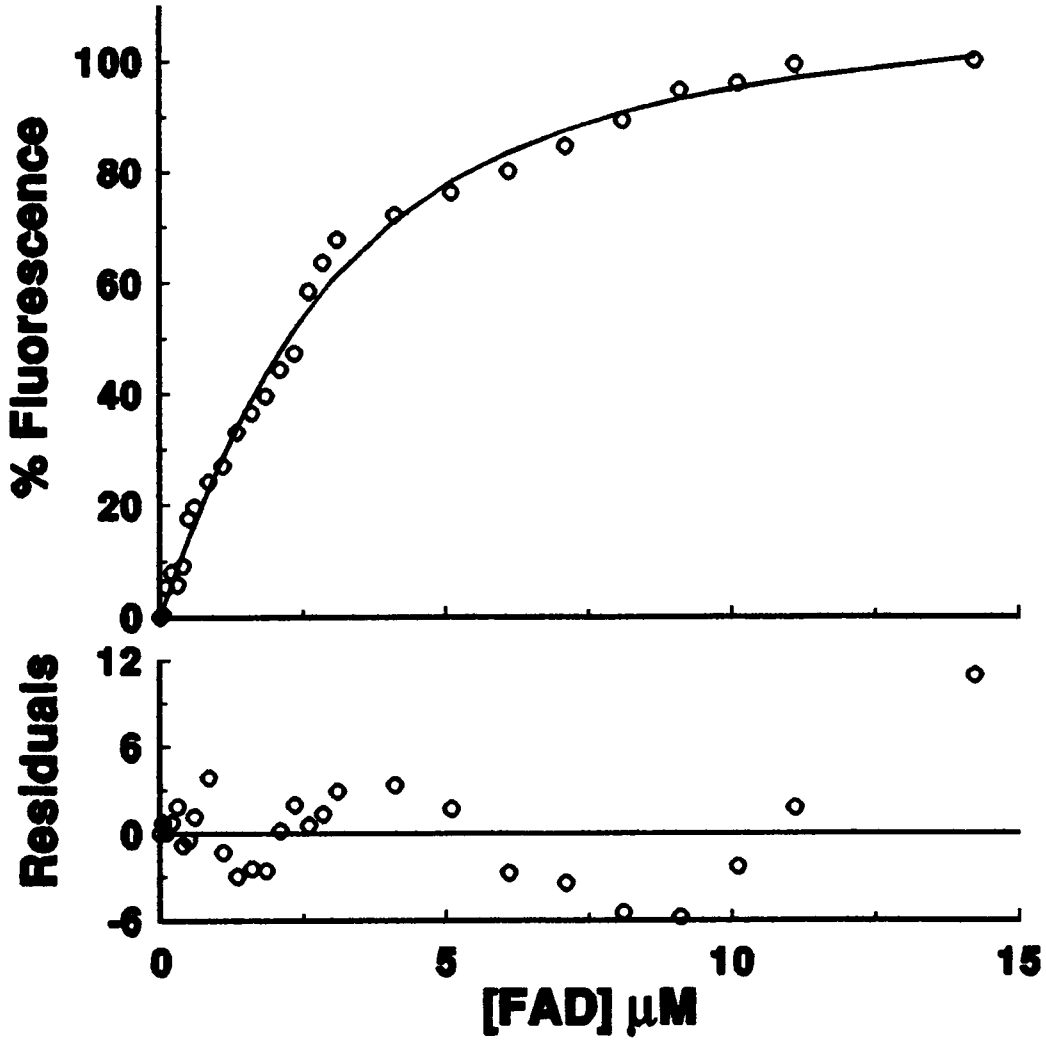

Figure 20: Fluorescence enhancement of the ligand FAD with R67 DHFR. Experiment was performed using an excitation wavelength of 450 nm and an emission wavelength of 540 nm.

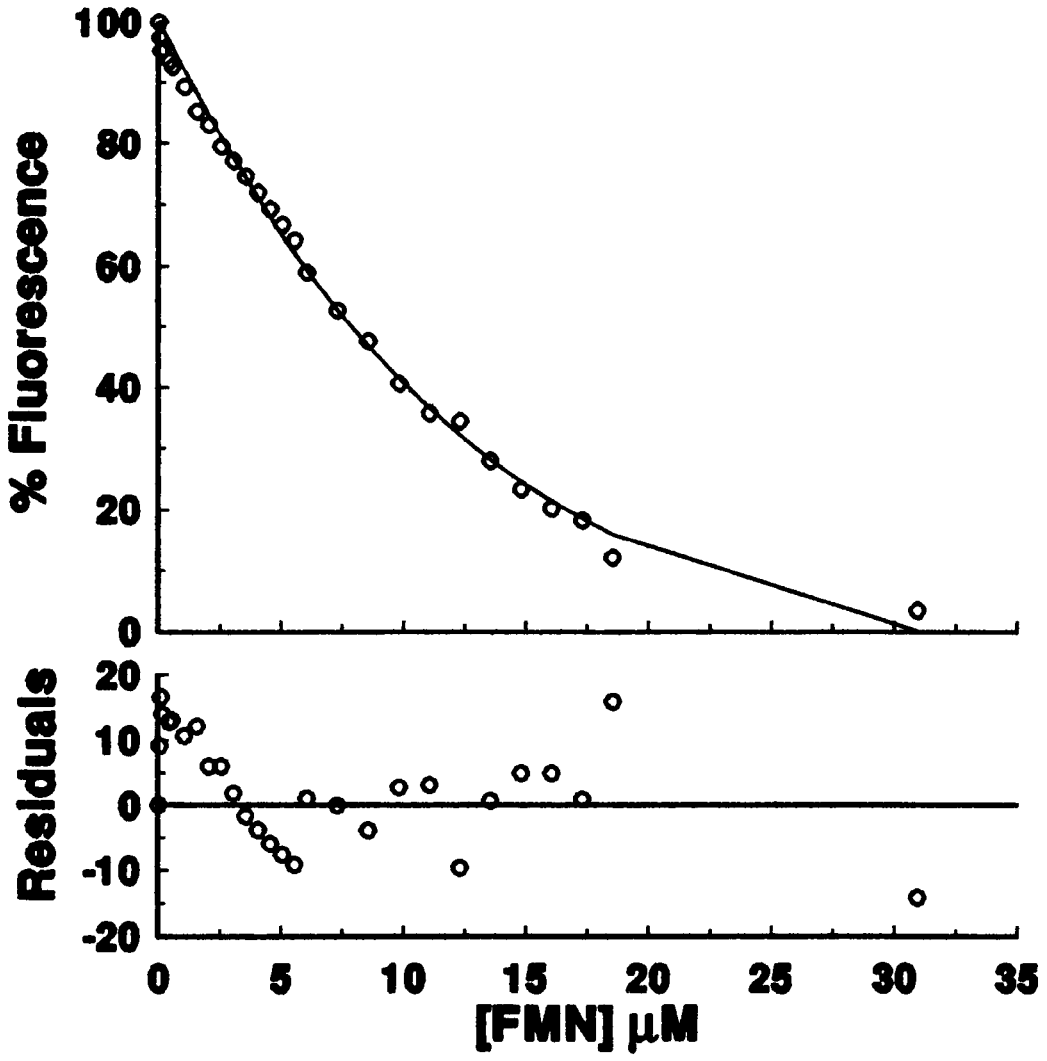

Figure 21: Fluorescence quenching of tryptophan residues in R67 DHFR using FMN as the ligand. Experiment was performed using an excitation wavelength of 290 nm and emission wavelength of 340 nm.

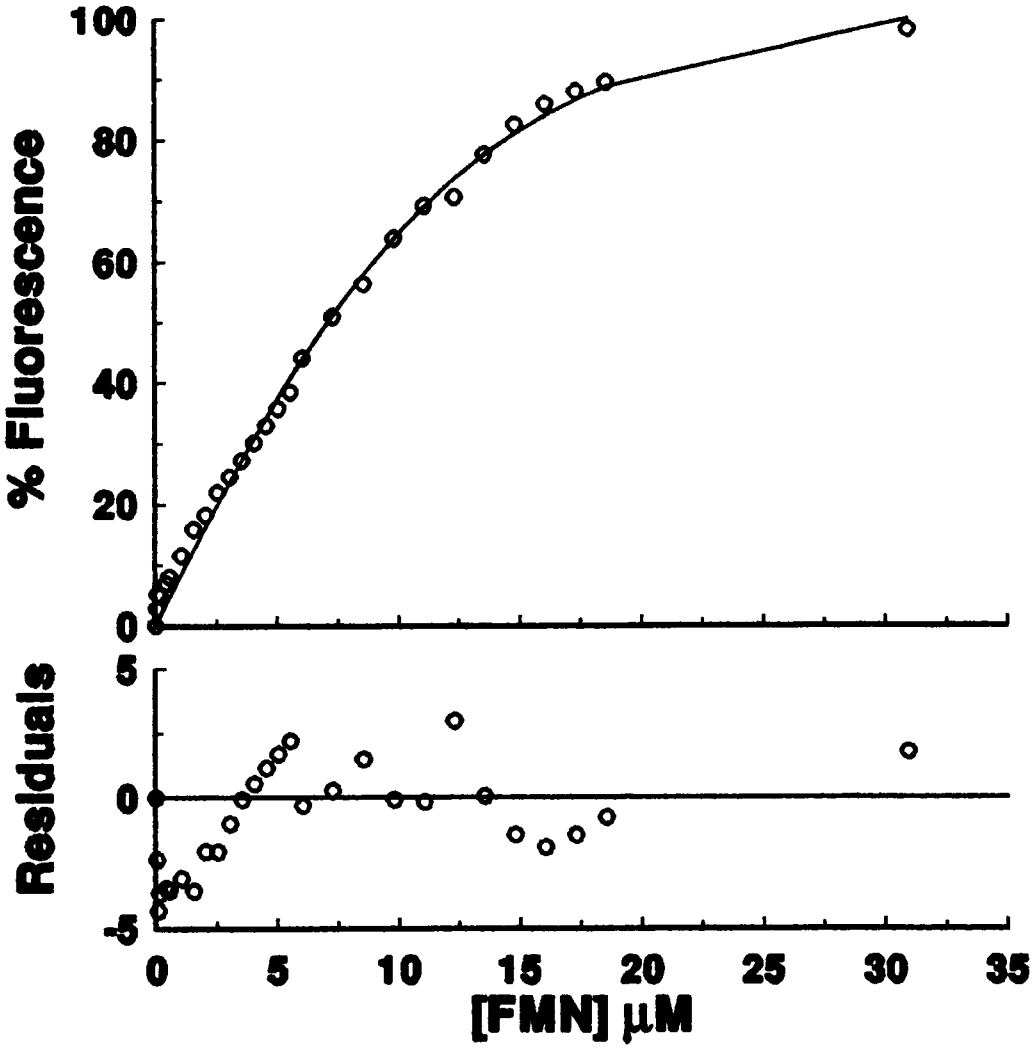

Figure 22: Fluorescence enhancement of the ligand FMN with R67 DHFR. Experiment was performed using an excitation wavelength of 366 nm and an emission wavelength of 527 nm.

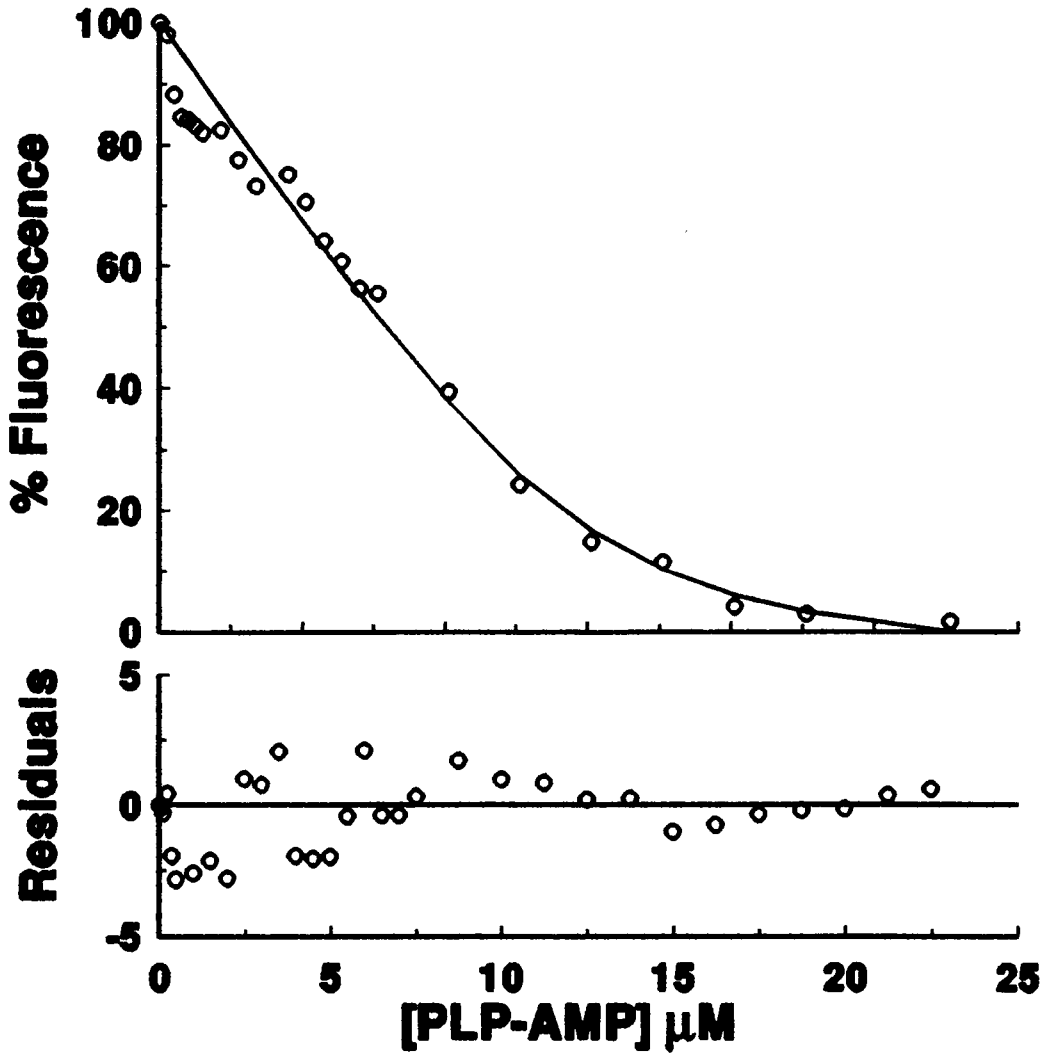

Figure 23: Fluorescence quenching of tryptophan residues in R67 DHFR using PLP-AMP. Experiment was performed using an excitation wavelength of 290 nm and an emission wavelength of 340 nm.

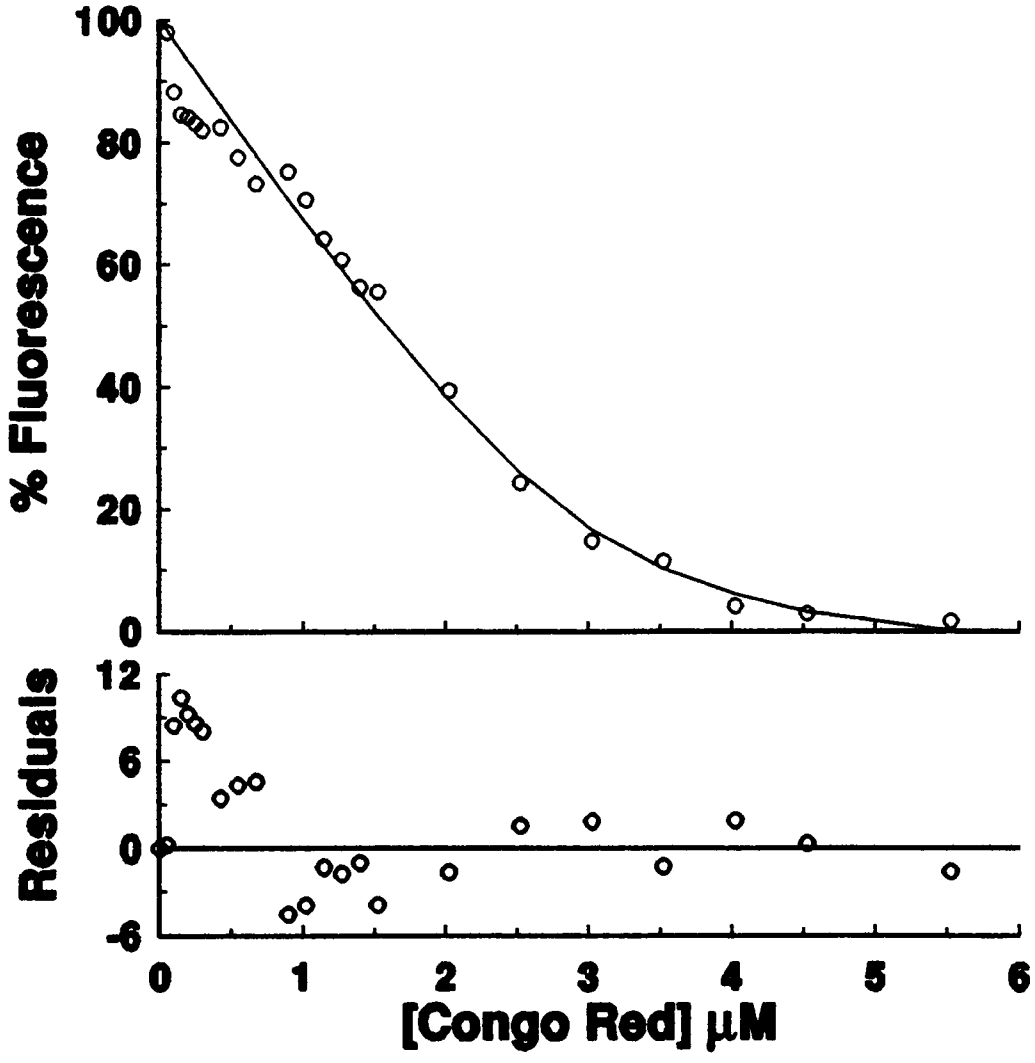

Figure 24: Fluorescence quenching of tryptophan residues in R67 DHFR using congo red as the ligand. Experiment was performed using an excitation wavelength of 290 nm and an emission wavelength of 340 nm.

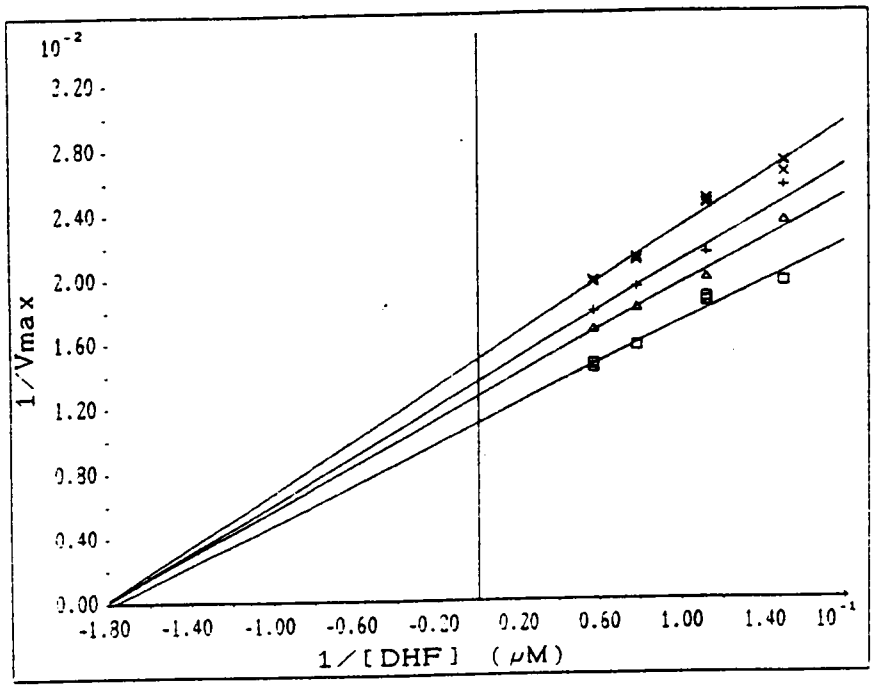

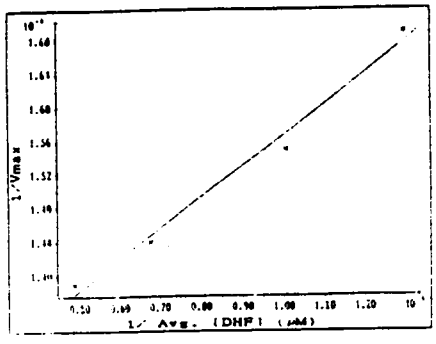

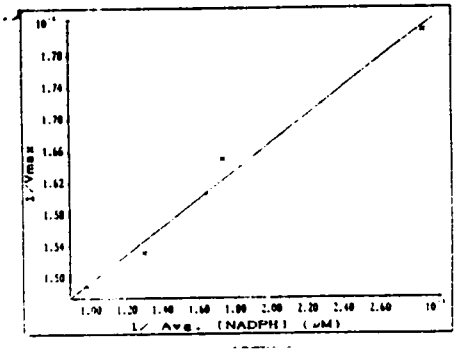

Figure 25: Michaelis-Menten subsaturating kinetics from the R67 $DHFR_{double}$ catalyzed reduction of DHF.

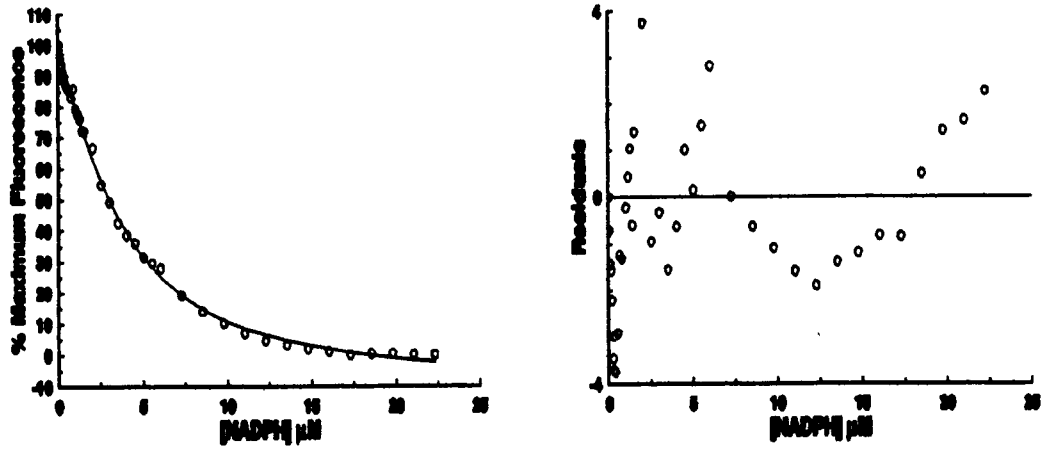

R67 native

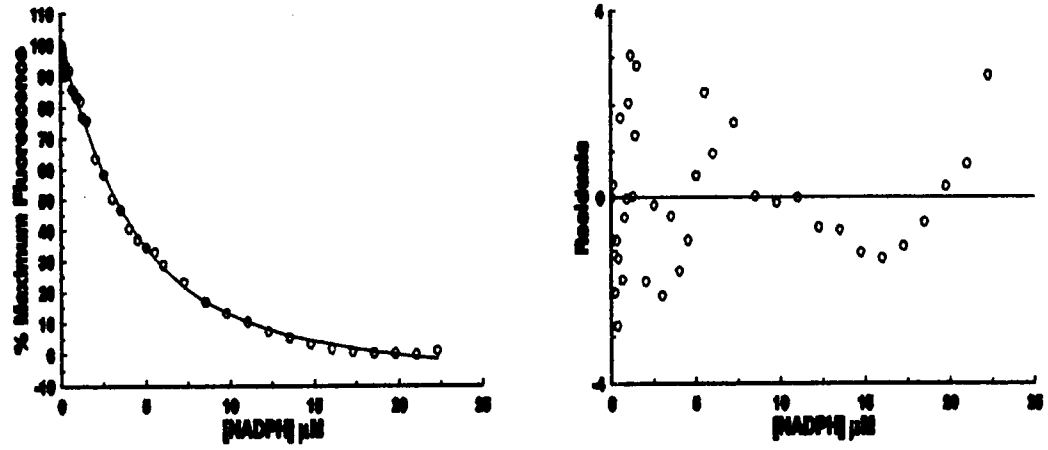

R67 double

Figure 26: Fluorescence quenching of tryptophan residues of R67 $DHFR_{double}$ and R67 $DHFR_{native}$ using NADPH as the ligand. Experiment was performed with an excitation wavelength of 290 nm and an emission wavelength of 340 nm.

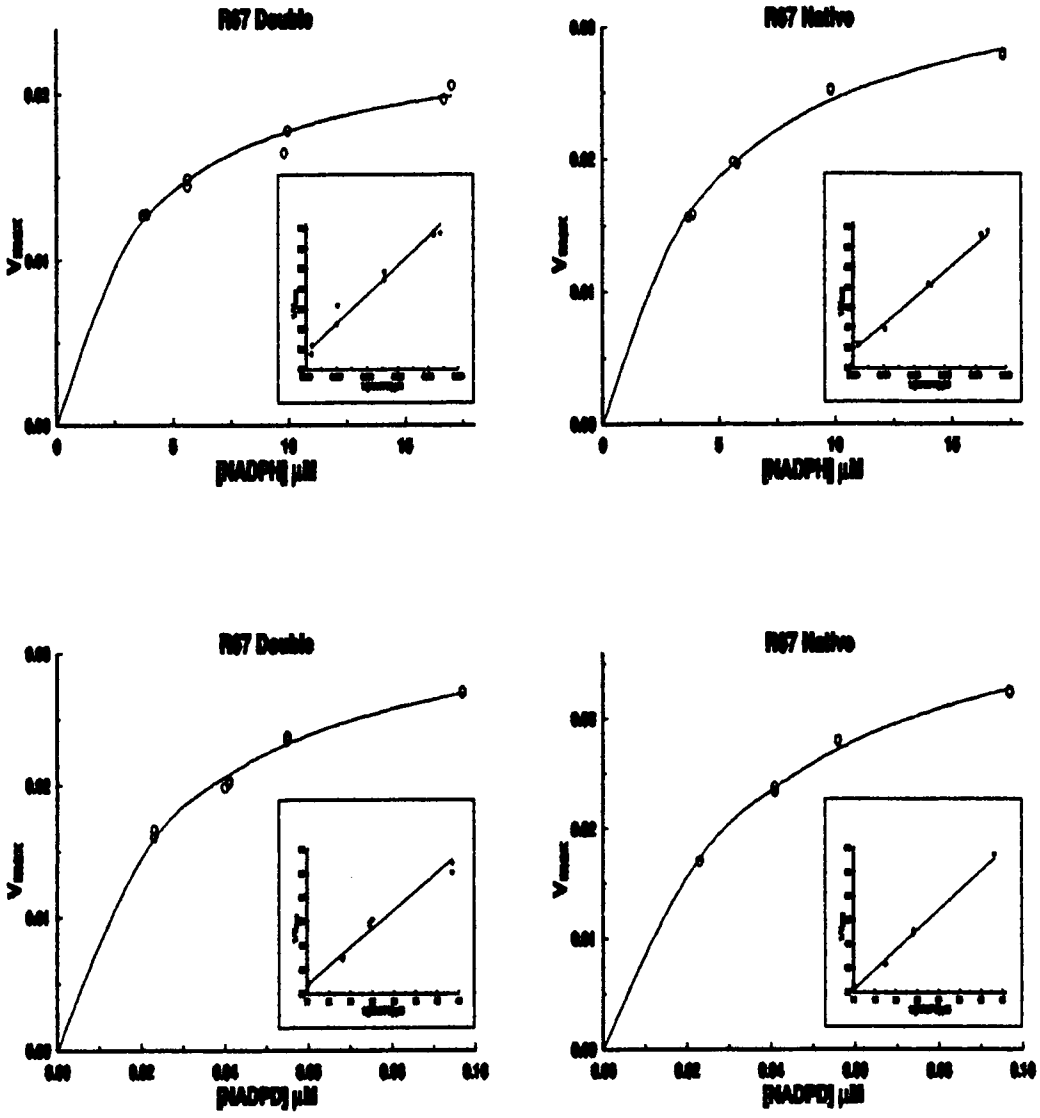

Figure 27: Michaelis-Menten kinetics from the R67 $DHFR_{double}$ and R67 $DHFR_{native}$ reduction of DHF using NADPD or NADPH as the cofactor.

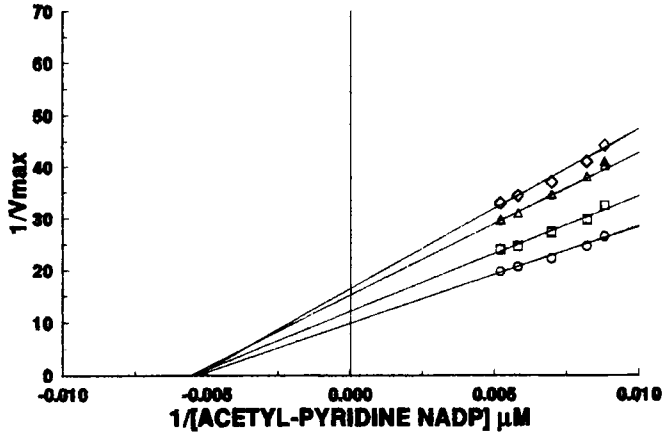

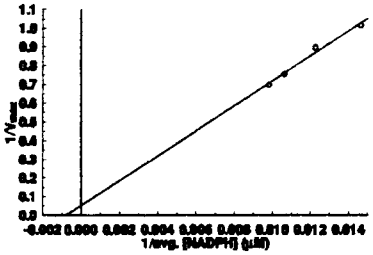

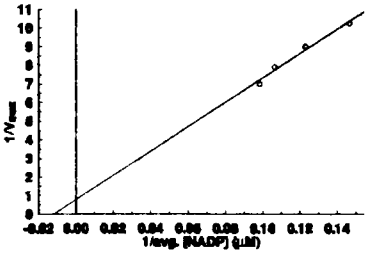

Figure 28: Michaelis-Menten subsaturating kinetics from the H62C R67 DHFR catalyzed reaction with acetyl-pyridine $NADP^+$ and NADPH.

TABLE 1

EXTINCTION COEFFICIENTS AND pKa VALUES FOR DHF, q-DMP, AND MTHF

SUBSTRATE	EXTINCTION COEFF. (cm^{-1} M^{-1} X 10^4)	pKa VALUE
DHF[1] (@340 nm)	7.72	2.59
q-DMP[2](@ 303 nm)	6.21	5.15
MTHF[3] (@ 297 nm)	3.2	3.2
DCPIP[4] (@ 515 nm)	1.5	5.57

1-Poe, 1977 2-Kaufman, 1987 3- Kallen, 1972 4- Gurr, 1960

TABLE 2

KINETIC PARAMETERS FOR THE R67 DHFR CATALYZED REDUCTION OF DHF

ENZYME USED	k_{cat} (sec-1)	$K_{m(DHF)}$ (μM)	$K_{m(NADPH)}$ (μM)
R67 DHFR DATA	1.1 ± 0.03	6.9 ± 0.9	3.1 ± 0.2
R67 DHFR LITERATURE	1.3	5.8	3.0

Note: Experiment was performed in a MET buffer at pH of 7.0.
Source of literature values: Reece *et al.*, 1992

TABLE 3

KINETIC PARAMETERS FOR THE R67 DHFR CATALYZED REDUCTION OF q-DMP

ENZYME USED	k_{cat} (sec-1)	$K_{m(q\text{-}DMP)}$ (μM)	$K_{m(NADPH)}$ (μM)
R67 DHFR DATA	0.8 ± 0.03	154 ± 0.9	6.9 ± 0.2
DHPR DATA	0.9 ± 0.04	13.5 ± 1.6	6.7 ± 0.8
DHPR LITERATURE	1.1	15.2	5.7

Note: Experiment was performed in a MET buffer at pH 7.0. DHPR control kinetics were done using NADH as the cofactor. Source of literature values: Craine, *et al.*, 1972

TABLE 4

KINETIC PARAMETERS FOR THE R67 DHFR CATALYZED REDUCTION OF MTHF

ENZYME USED	k_{cat} (sec-1)	$K_{m(MTHF)}$ (μM)	$K_{m(NADPH)}$ (μM)
R67 DHFR DATA	0.8 ± 0.03	78 ± 10	7.1 ± 0.7
MTHFR DATA	≥ 11.3	6.8 ± 0.4	18.9 ± 1.6
MTHFR LITERATURE	16.7	5.5	16.0

Note: Experiments were performed anaerobically in a MET buffer at pH of 7.0. Wt. *E. coli* DHFR was also attempted, but found to be unable to reduce the substrate. Kinetic parameters determined for the MTHFR catalyzed reduction were performed using an impure protein received from R. Matthews. Source of literature values: Matthews, and Haywood, 1973

TABLE 5

KINETIC PARAMETERS FOR THE R67 DHFR CATALYZED REDUCTION OF DHB

ENZYME USED	k_{cat} (sec-1)	$K_{m(DHB)}$ (μM)	$K_{m(NADPH)}$ (μM)
R67 DHFR DATA	0.9 ± 0.2	21.8 ± 1.6	7.2 ± 0.9
Wt. *E.coli* DHFR DATA	2.4 ± 0.4	46.3 ± 3.6	2.8 ± 0.8
Wt. chicken DHFR LITERATURE	3.6	30	1.1

Note: Experiments were performed in a MET buffer at pH 7.0.

TABLE 6

KINETIC PARAMETERS FOR THE R67 DHFR CATALYZED REDUCTION OF DCPIP

ENZYME USED	k_{cat} (sec^{-1})	$K_{m(DCPIP)}$ (μM)	$K_{m(NADPH)}$ (μM)
R67 DHFR	0.4 ± 0.1	33 ± 0.6	5.3 ± 0.1

Note: Experiments were performed in MET buffer pH 7.0 which was devoid of ß-Me. *E. coli* chromosomal DHFR was also attempted and found not to utilize DCPIP.

TABLE 7

KINETIC ISOTOPE PARAMETERS FOR THE R67 DHFR AND THE Wt. *E.coli* DHFR CATALYZED REDUCTION OF DHB

ENZYME USED	k_{cat} (sec-1) (NADPH)	K_{cat} (sec-1) (NADPD)	^{D}V values
R67 DHFR DATA	0.9 ± 0.1	0.2 ± 0.01	3.7
Wt. E.coli DHFR DATA	2.1 ± 0.04	1.1 ± 0.1	2.3

TABLE 8

FLUORMETRIC PARAMETERS OF R67 DHFR USING FAD AND FMN

LIGAND USED	K_d (μM)	R_o	BINDING STOICHOMETRY
FAD 290/340	1.53	2.03	0.34
FAD 450/540	1.61	2.25	0.37
FMN 290/340	3.32	16.62	3.31
FMN 366/527	3.46	18.94	3.73

Note: Wt. chromosomal *E. coli* DHFR has been found to be unable to bind either FAD or FMN

TABLE 9

FLUOROMETRIC PARAMETERS OF R67 DHFR WITH PLP-AMP AND CONGO RED

LIGAND USED	K_d (μM)	R_o	BINDING STOICHOMETRY
PLP-AMP	65	15.41	5.1
Congo Red	246	3.83	1.3

Note: Wt. chromosomal *E. coli* DHFR has been found to be unable to bind either FAD or FMN

TABLE 10

KINETIC PARAMETERS FOR THE R67 $DHFR_{double}$ CATALYZED REDUCTION OF DHF

ENZYME USED	k_{cat} (sec-1)	$K_{m(DHF)}$ (μM)	$K_{m(NADPH)}$ (μM)
R67 $DHFR_{double}$ DATA	1.1 ± 0.09	6.3 ± 1.1	2.8 ± 0.5
R67 $DHFR_{native}$ DATA	1.1 ± 0.03	6.9 ± 0.9	3.1 ± 0.2
R67 $DHFR_{native}$ LITERATURE	1.3	5.8	3.0

Note: Experiments were performed in a MET buffer at pH 7.0.

TABLE 11

FLUOROMETRIC PARAMETERS FOR THE R67 $DHFR_{double}$ BINDING NADPH

LIGAND USED	K_d	R_o	BINDING STOICHOMETRY
NADPH	2.1	32	1.2

TABLE 12

KINETIC ISOTOPE PARAMETERS FOR THE R67 DHFR AND THE R67 $DHFR_{double}$ CATALYZED REDUCTION OF DHF

ENZYME USED	k_{cat} (sec-1) (NADPH)	K_{cat} (sec-1) (NADPD)	^{D}V values
R67 $DHFR_{double}$ DATA	0.9 ± 0.04	0.3 ± 0.02	3.0
R67 $DHFR_{native}$ DATA	1.0 ± 0.1	0.3 ± 0.01	3.0

TABLE 13

KINETIC PARAMETERS FOR THE H62C R67 DHFR CATALYZED REDUCTION OF ACETYL-PYRIDINE $NADP^+$ AND NADPH

ENZYME USED	k_{cat} (sec-1)	$K_{m(NADP+)}$ (μM)	$K_{m(NADPH)}$ (μM)
H62C R67 DHFR DATA	0.4 ± 0.08	18 ± 0.9	6.7 ± 0.2

Note: Experiment was performed in a MET buffer at pH 7.0 devoid of ß-Me. Native R67 DHFR kinetics were also attempted, however R67 DHFR was unable to utilize acetyl-pyridine $NADP^+$.

TABLE 14

KINETIC PARAMETERS FOR THE DHPR CATALYZED REDUCTION OF MTHF

SOURCE	k_{cat} (sec^{-1})	$Km_{MTHF\ OR\ q-DHP}$ (μM)	$Km_{NADH\ OR\ NADPH}$ (μM)
$DHPR_{DATA}$ (MTHF)	0.3 ± 0.04	89.6 ± 3.6	7.3 ± 0.4
R67 $DHFR_{DATA}$ (MTHF)	0.8 ± 0.1	78.1 ± 10	7.1 +0.7
$DHPR_{CONTROL}$ (q-DHP)	0.8 ± 0.04	13.5 ± 1.6	6.7 ± 0.8

VITAE

Janel Christine Holland was born in Cheektowaga, New York on March 12, 1968. She was raised in Lancaster, New York where she attended and graduated from Lancaster Central High School in June of 1986. She then attended the State University of New York, College at Fredonia. In May of 1990 graduated with two Bachelor of Science Degrees, one in Recombinant Gene Technology and the second in Chemistry. In August of 1990 she enrolled as a graduate student in Biochemistry, at The University of Tennessee, Knoxville, and in December of 1993 graduated with a Masters of Science Degree in Biochemistry.